Available online at www.sciencedirect.com

ScienceDirect

Information Fusion 00 (2024) 1–22

Information Fusion

Distributed Fusion Filtering for Multi-sensor Nonlinear Networked Systems with Multiple Fading Measurements via Stochastic Communication Protocol

Jun Hu[a,b,*], Zhibin Hu[a,c], Raquel Caballero-Águila[d], and Xiaojian Yi[e,f]

[a] *Department of Applied Mathematics, Harbin University of Science and Technology, Harbin 150080, China.*

[b] *School of Automation, Harbin University of Science and Technology, Harbin 150080, China.*

[c] *School of Mathematics and Statistics, Jining Normal University, Ulanqab 012000, China.*

[d] *Departamento de Estadística, Universidad de Jaén, Paraje Las Lagunillas, 23071 Jaén, Spain.*

[e] *School of Mechatronical Engineering, Beijing Institute of Technology, Beijing 100081, China.*

[f] *Yangtze Delta Region Academy of Beijing Institute of Technology, Jiaxing 314003, China.*

[*] *Corresponding author. E-mail:* jhu@hrbust.edu.cn

Abstract

This paper studies the distributed fusion filtering (DFF) issue for a class of nonlinear delayed multi-sensor networked systems (MSNSs) subject to multiple fading measurements (MFMs) under stochastic communication protocol (SCP). The phenomenon of MFMs occurs randomly in the network communication channels and is characterized by a diagonal matrix with certain statistical information. In order to decrease the overload of communication network and save network resources, the SCP that can regulate the information transmission between sensors and estimators is adopted. The primary aim of the tackled problem is to develop the DFF method for nonlinear delayed MSNSs in the presence of MFMs and SCP based on the inverse covariance intersection fusion rule. In addition, the local upper bound (UB) of the filtering error covariance (FEC) is derived and minimized by means of suitably designing the local filter gain. Moreover, the boundedness analysis regarding the local UB is proposed with corresponding theoretical proof. Finally, two simulation examples with comparative illustrations are given to display the usefulness and feasibility of the derived theoretical results.

Keywords: Distributed fusion filtering, Time-varying nonlinear delayed systems, Multiple fading measurements, Stochastic communication protocol, Inverse covariance intersection fusion

Acronyms

1. Introduction

Over the past years, the study of SNs has stirred significant interest of many researchers, and meaningful results have been proposed with wide application domains including area monitoring, health care monitoring, environmental sensing, and target tracking, see [1, 2, 3, 4]. Recently, some methods have been proposed to estimate the system states observed by sensors [5, 6]. Most notably, the information fusion estimation, which means that the fusion estimator

SNs	sensor networks
DFF	distributed fusion filtering
WM	weighting matrix
ICI	inverse covariance intersection
LFM	Lyapunov functional method
FWMM	free-weighting matrix method
MSNSs	multi-sensor networked systems
CI	covariance intersection
MFMs	multiple fading measurements
NRSM	network resource scheduling mechanism
DETM	dynamic event-triggered mechanism
RRP	Round-Robin protocol
RAP	random access protocol
SCP	stochastic communication protocol
FEC	filtering error covariance
UB	upper bound
LF	local filter
IID	independent and identically distributed
PEC	prediction error covariance
MSE	mean square error

can be derived in terms of the measurement information from multiple sensors, has been extensively used in many fields due to its advantages of high measurement accuracy and easy-to-operate feature, especially in the target tracking and unmanned ground vehicle [7]. Generally speaking, there are many fusion strategies, such as centralized fusion filtering, DFF, and sequential fusion filtering, see [8, 9, 10, 11, 12, 13]. Among them, the DFF approach has been widely utilized due to the fact that it has strong robustness and fault tolerance in information fusion estimation domain. Furthermore, in order to obtain improved estimation results regarding the fusion filter, a considerable amount of effort has been made and several fusion rules have been presented, for example, the WM fusion method, ICI fusion method, and CI fusion method [10, 14, 15].

In practical engineering systems, the time-delay is a very widespread phenomenon, which may lead to divergence and system instability. Accordingly, some approaches have been presented to mitigate the impact of time-delay, including the LFM, FWMM, delay decomposition method and multiple integral functional method, see [16, 17]. Furthermore, it is noteworthy that the time-delay has been taken into account when handling the state estimation problem over SNs. On the one hand, as the information is transmitted through the SNs, the measurements may be randomly delayed when they are received by the remote signal receiver. In order to handle this issue, some approaches have been presented, such as the methods of the augmentation and prediction compensation. For example, the algorithms of the distributed filtering and DFF have been respectively proposed in [18, 19] for linear systems over SNs with random sensor delays. On the other hand, when the design problem of the estimation algorithm for dynamic systems with time-delay over SNs becomes a concern, a key issue is how to construct the local estimator under the influence of time-delay. For instance, the fault estimation method has been provided in [20] for a class of delayed systems with multiple agents, where the delay-dependent stability conditions have been provided by means of the LFM and FWMM. Furthermore, the estimation issues have been addressed in [21, 22] for nonlinear delayed MSNSs. More specifically, a filtering algorithm with the distributed structure has been presented for continuous nonlinear delayed MSNSs with switching topology, where the stability problem of the addressed systems has been discussed in terms of the average dwell time strategy and LFM. So far, unfortunately, the DFF problem for nonlinear delayed MSNSs has not been widely studied, which constitutes one of the motivations of this study.

Notice that the transmitted information is affected by unreliable networked environment in communications, which will cause the network-induced phenomena [23, 24, 25, 26]. For example, an effective scheme has been given in [27] to handle the missing data and provide the measurement selection as well as power allocation method in distributed multi-target tracking domain. It is worth noting that the measurement may randomly degrade during the transfer process and the missing measurements can be considered as a special case of fading ones [24]. Accordingly, much effort has been

made to investigate the filtering problem subject to missing measurements and some results have been published [9, 28, 29]. Furthermore, the state estimation schemes have been extensively given in [30, 31] for stochastic nonlinear systems with multiple missing measurements. In the context of the above discussion, it is noteworthy that the random variable governed by the Bernoulli distribution has been generally utilized to describe the missing measurement phenomenon, which shows that the received measurement information only includes two cases, namely, complete information and complete loss. Nevertheless, the above-mentioned case is inadequate for modelling the fading measurements in practice, which has stirred much attention. For instance, the filtering scheme has been provided in [32] for stochastic nonlinear systems subject to random parameter matrices and fading measurements, where the estimator has been given by means of the innovation analysis method. In view of the results in [32], a filtering approach has been developed in [33] for nonlinear systems with MFMs and random parameter matrices, which further extends its application field. In multi-sensor systems, furthermore, the distributed filtering and fusion estimation algorithms have been respectively implemented in [18, 34] for linear systems with fading measurements. Up to now, nevertheless, the DFF problem has not been comprehensively tackled for nonlinear MSNSs with MFMs, which requires additional consideration.

In practice, the SNs usually consist of many sensor nodes with the abilities of sensing and communication. Accordingly, the development and utilization of the SNs frequently encounter network congestion, huge waste of network resources, and performance degradation owing to the fact that the network is restricted by limited bandwidth and hardware level [35, 36, 37]. In order to reasonably use the network resources as well as decrease the network overload, the NRSM regarding as an effective method has been taken into account during the network transmission, which can determine whether the current sensor node is allowed to transfer data at every moment [38, 39, 40]. In industry, there exist several well-known NRSMs including DETM, RRP, RAP, SCP and so on. Recently, it is worth noting that plenty of effort has been taken to tackle the estimation problem for MSNSs under the NRSM, which causes a good deal of literature to be reported, see [41, 42, 43, 44, 45, 46, 47]. For example, the H_∞ estimation problem has been examined in [42] for complex networks with intermittent nonlinearity under the RRP, where the performance of the derived estimator has been discussed. Based on SCP, moreover, the H_∞ estimation algorithms have been developed in [43, 41] for genetic regulatory networks and memristive neural networks, respectively. Very recently, new DFF scheme handling the gain perturbations and the limitation issue of the network bandwidth has been presented in [31]. So far, however, the issue of the DFF has been rarely examined for MSNSs under the SCP, let alone the situation when the nonlinear time-delay as well as MFMs are considered simultaneously.

In this paper, on the basis of the preceding discussions, our goal is to present an SCP-based DFF scheme for nonlinear delayed MSNSs with MFMs. When the transmitted information is received by a remote estimator via data-transmission channels, the SCP is used to lighten the burden of transmission and the MFMs can reflect the case that the network channel is affected by degradation. Furthermore, the essential difficulties are summarized as follows: (i) how to develop an effective fusion filtering algorithm that mitigates the impacts of MFMs, time-delay and SCP; and (ii) how to present an appropriate method to guarantee the boundedness on the FEC. Accordingly, the corresponding research is presented to tackle the above difficulties. The primary contributions are that: 1) a new DFF algorithm is developed for a class of nonlinear delayed MSNSs subject to MFMs and SCP according to the ICI fusion criterion; 2) the expression of the UB concerning the FEC is presented, where the UB can be minimized through selecting the appropriate LF gain; and 3) a sufficient condition is given for developed DFF algorithm, under which the UB on the FEC is bounded uniformly.

Notations: $\mathbb{R}^n$ denotes the n-dimensional Euclidean space. $\|f\|$ represents the Euclidean norm of a vector f. S^{-1} and S^T refer to inverse and transpose of the matrix S, respectively. For the matrix D, $\lambda_{\max}(D)$ stands for its maximum eigenvalue. $\delta(\cdot) \in \{0,\ 1\}$ denotes for the Kronecker delta function. For the matrix B, $\mathrm{tr}(B)$ denotes its trace. $\mathrm{Prob}\{\cdot\}$ denotes occurrence probability of event "$\cdot$". For the random variable z, $\mathbb{E}\{z\}$ denotes its mathematical expectation. I stands for the identity matrix with appropriate dimension. $J_{r\times s}$ refers to the $r \times s$ all-ones matrix. 0 denotes the zero matrix with appropriate dimension. $A \succ B (A \succeq B)$ denotes that $A - B$ is positive (semi-positive) definite, where A and B are symmetric matrices. The symbol "$\circ$" represents the Hadamard product.

2. Problem Formulation and Preliminaries

In this paper, we consider the following class of time-varying nonlinear delayed MSNSs:

$$\vec{\mathrm{x}}_{\mu+1} = \vec{A}_\mu \vec{\mathrm{x}}_\mu + \vec{f}(\vec{\mathrm{x}}_{\mu-d}) + \vec{B}_\mu \vec{w}_\mu \tag{1}$$

$$\vec{y}_{i,\mu} = \Theta_{i,\mu}\vec{C}_{i,\mu}\vec{\mathrm{x}}_\mu + \vec{v}_{i,\mu},\ i = 1, 2, \cdots, L \tag{2}$$

where $\vec{\mathrm{x}}_\mu \in \mathbb{R}^n$ denotes the system state, and its initial value is $\vec{\mathrm{x}}_0$ with mean $\bar{\vec{\mathrm{x}}}_0$ and covariance $\vec{P}_{0|0} \succ 0$, $\vec{y}_{i,\mu} \in \mathbb{R}^{q_i}$ is the measurement output of the ith sensor. $\vec{w}_\mu \in \mathbb{R}^p$ and $\vec{v}_{i,\mu} \in \mathbb{R}^{q_i}$ are uncorrelated Gaussian white noises, and these noises have zero means and covariances $\vec{Q}_\mu$ and $R_{i,\mu} \succ 0$, respectively. $\vec{f}(\cdot)$ is the nonlinear function with the continuous differentiability. $d > 0$ is a known integer describing the time-delay. $\vec{A}_\mu$, $\vec{B}_\mu$ and $\vec{C}_{i,\mu}$ are known matrices of appropriate dimensions. $\Theta_{i,\mu} := \mathrm{diag}\left\{\theta_{i,\mu}^{(1)}, \theta_{i,\mu}^{(2)}, \cdots, \theta_{i,\mu}^{(q_i)}\right\}$ with $\theta_{i,\mu}^{(m)}$ $(m = 1, 2, \cdots, q_i)$ being q_i independent random variables. L represents the number of sensors.

The phenomenon of the MFMs from different channels is governed by the random variables $\theta_{i,\mu}^{(m)}$ $(m = 1, 2, \cdots, q_i)$ taking values on the closed interval $[0, 1]$ and satisfying:

$$\mathbb{E}\left\{\theta_{i,\mu}^{(m)}\right\} = \bar{\theta}_{i,\mu}^{(m)},\ \ \mathrm{Cov}\left\{\theta_{i,\mu}^{(m)}\right\} = \rho_{i,\mu}^{(m)},$$

where $\bar{\theta}_{i,\mu}^{(m)}$ and $\rho_{i,\mu}^{(m)}$ are given positive scalars. Significantly, it is usually assumed that the measurement noise is independent of the fading matrix, as they are caused by different factors and follow different statistical characteristics.

Note that the information collision may occur in the data transmission with the increase of the number of sensors. The use of SCP between local sensors and local estimators can reduce the information overload and save energy. According to the results from literature [41, 43], it is allowed that only one sensor node can transmit its data at each moment. To further illustrate the influence of the SCP, let $\kappa_\mu \in \{1, 2, \cdots, L\}$ be the selected sensor node, which can transmit information in network environment at moment μ. Here, $\{\kappa_\mu\}_{\mu>0}$ denote random variables that are assumed to be mutually IID. The occurrence probability of $\kappa_\mu = i$ can be described by:

$$\mathrm{Prob}\left\{\kappa_\mu = i\right\} = p_i,$$

where $p_i \in (0, 1]$ $(i \in 1, 2, \cdots, L)$ stands for the probability of the ith sensor to be chosen to transmit information and $\sum_{i=1}^{L} p_i = 1$. In the following context, we assume that $\vec{w}_\mu$, $\vec{v}_{i,\mu}$, $\Theta_{i,\mu}$, κ_μ and $\vec{\mathrm{x}}_0$ are mutually independent.

Let $y_{i,\mu}$ be the local measurement output received by the ith estimator at time μ. In the light of the zero-order holder strategy, the updating rule of $y_{i,\mu}$ under the SCP strategy is expressed by:

$$y_{i,\mu} = \begin{cases} \vec{y}_{i,\mu}, & \text{if } i = \kappa_\mu, \\ y_{i,\mu-1}, & \text{otherwise.} \end{cases} \tag{3}$$

According to (3), we have

$$y_{i,\mu} = \kappa_\mu^i \vec{y}_{i,\mu} + (1 - \kappa_\mu^i) y_{i,\mu-1}, \tag{4}$$

where $\kappa_\mu^i = \delta(\kappa_\mu - i)$.

Remark 1 *It is important to note that the addressed time-delay problem is distinct from other related problems, such as out-of-sequence measurements and asynchronous problems. Out-of-sequence measurements refer to cases where the order of measurements received by an estimator does not match the time order in which they were taken. Asynchronous problems, on the other hand, generally involve discrepancies in the timing or synchronization of data acquisition in a system. The addressed time-delay problem in this paper focuses on the development of the fusion estimation algorithm that can accurately estimate the state of the time-delay system, rather than issues related to the order or synchronization of measurements.*

Remark 2 *It is noteworthy to mention that there exist some communication protocols that have been investigated in networked systems, including RRP, SCP and RAP [42, 43, 44, 45, 46]. Among them, RAP and SCP are also considered*

as same class of communication protocols, which can be usually described by the IID random variables or Markov chain [47]. Although this protocol can reduce the information overload and save energy, there may be instances where measurement data cannot be transmitted in a timely manner when $i \neq k_\mu$. If we only consider measurement missing without taking any other ways, it may lead to degraded system performance or instability. For such case, in order to obtain more effective information, several compensation methods can be adopted at the receiving end, such as the zero-order holder method and zero-input method. Compared with the latter one, the zero-order holder method has higher estimation precision due to the ability to utilize the information at certain moments. In this paper, SCP is adopted for nonlinear delayed MSNSs, which can alleviate the traffic congestion caused by information transmission and save network resources. In addition, $\{\kappa_\mu\}_{\mu>0}$ represent the stochastic process of IID random variables, which can be used to depict the scheduling method of SCP. Consequently, the received sensor measurement information, which satisfies the update strategy (3), can be characterized by (4).

Taking (4) into consideration, the system (1)-(2) subject to the SCP can be reconstructed as follows:

$$\mathsf{x}_{\mu+1} = A_\mu \mathsf{x}_\mu + f(\mathsf{x}_{\mu-d}) + B_\mu w_\mu, \tag{5}$$
$$y_{i,\mu} = C_{i,\mu}\mathsf{x}_\mu + \kappa_\mu^i v_{i,\mu}, \tag{6}$$

where

$$\mathsf{x}_{\mu+1} = \begin{bmatrix} \vec{\mathsf{x}}_{\mu+1} \\ y_{i,\mu} \end{bmatrix}, \quad f(\mathsf{x}_{\mu-d}) = \begin{bmatrix} \vec{f}(\vec{\mathsf{x}}_{\mu-d}) \\ 0 \end{bmatrix}, \quad A_\mu = \begin{bmatrix} \vec{A}_\mu & 0 \\ \kappa_\mu^i \Theta_{i,\mu}\vec{C}_{i,\mu} & (1-\kappa_\mu^i)I \end{bmatrix},$$
$$B_\mu = \begin{bmatrix} \vec{B}_\mu & 0 \\ 0 & \kappa_\mu^i I \end{bmatrix}, \quad w_\mu = \begin{bmatrix} \vec{w}_\mu \\ \vec{v}_{i,\mu} \end{bmatrix}, \quad C_{i,\mu} = \begin{bmatrix} \kappa_\mu^i \Theta_{i,\mu}\vec{C}_{i,\mu} & (1-\kappa_\mu^i)I \end{bmatrix}, \quad v_{i,\mu} = \vec{v}_{i,\mu}.$$

Define the following notations:

$$\bar{\Theta}_{i,\mu} = \mathbb{E}\{\Theta_{i,\mu}\} = \operatorname{diag}\left\{\bar{\theta}_{i,\mu}^{(1)}, \bar{\theta}_{i,\mu}^{(2)}, \cdots, \bar{\theta}_{i,\mu}^{(q_i)}\right\},$$
$$\tilde{\Theta}_{i,\mu} = \Theta_{i,\mu} - \bar{\Theta}_{i,\mu} = \operatorname{diag}\left\{\tilde{\theta}_{i,\mu}^{(1)}, \tilde{\theta}_{i,\mu}^{(2)}, \cdots, \tilde{\theta}_{i,\mu}^{(q_i)}\right\},$$
$$\mathbb{E}\{\kappa_\mu^i\} = \Sigma_{j=1}^L p_j \delta(j-i) = p_i, \quad \mathbb{E}\{\kappa_\mu^i \kappa_\mu^j\} = p_i\delta(i-j),$$
$$\bar{A}_\mu = \mathbb{E}\left\{A_\mu\right\} = \begin{bmatrix} \vec{A}_\mu & 0 \\ p_i\bar{\Theta}_{i,\mu}\vec{C}_{i,\mu} & (1-p_i)I \end{bmatrix},$$
$$\tilde{A}_\mu = A_\mu - \bar{A}_\mu = \begin{bmatrix} 0 & 0 \\ (\kappa_\mu^i - p_i)\Theta_{i,\mu}\vec{C}_{i,\mu} + p_i\tilde{\Theta}_{i,\mu}\vec{C}_{i,\mu} & (p_i-\kappa_\mu^i)I \end{bmatrix}, \tag{7}$$
$$\bar{C}_{i,\mu} = \mathbb{E}\left\{C_{i,\mu}\right\} = \begin{bmatrix} p_i\bar{\Theta}_{i,\mu}\vec{C}_{i,\mu} & (1-p_i)I \end{bmatrix},$$
$$\tilde{C}_{i,\mu} = C_{i,\mu} - \bar{C}_{i,\mu} = \begin{bmatrix} (\kappa_\mu^i - p_i)\Theta_{i,\mu}\vec{C}_{i,\mu} + p_i\tilde{\Theta}_{i,\mu}\vec{C}_{i,\mu} & (p_i-\kappa_\mu^i)I \end{bmatrix}, \tag{8}$$
$$Q_\mu = \mathbb{E}\left\{w_\mu w_{\mathsf{k}}^T\right\} = \begin{bmatrix} \vec{Q}_\mu & 0 \\ 0 & R_{i,\mu} \end{bmatrix}\delta(\mu-\mathsf{k}), \quad B_\mu = \Upsilon_\mu \breve{B}_\mu, \tag{9}$$

with

$$\Upsilon_\mu = \begin{bmatrix} I & 0 \\ 0 & \kappa_\mu^i I \end{bmatrix}, \quad \breve{B}_\mu = \begin{bmatrix} \vec{B}_\mu & 0 \\ 0 & I \end{bmatrix}.$$

It can be seen that the mathematical expectations of $\tilde{\Theta}_{i,\mu}$, $\tilde{A}_\mu$ and $\tilde{C}_{i,\mu}$ are zero.

For the ith processor, the LF is constructed by:

$$\hat{\mathsf{x}}_{i,\mu+1|\mu} = \bar{A}_\mu \hat{\mathsf{x}}_{i,\mu|\mu} + f(\hat{\mathsf{x}}_{i,\mu-d|\mu-d}), \tag{10}$$
$$\hat{\mathsf{x}}_{i,\mu+1|\mu+1} = \hat{\mathsf{x}}_{i,\mu+1|\mu} + K_{i,\mu+1}(y_{i,\mu+1} - \bar{C}_{i,\mu+1}\hat{\mathsf{x}}_{i,\mu+1|\mu}), \tag{11}$$

where $\hat{\mathsf{x}}_{i,\mu+1|\mu}$ is the local predictor of the state, and $\hat{\mathsf{x}}_{i,\mu|\mu}$ stands for the local updated estimator of the state at time μ. The initial condition with respect to $\hat{\mathsf{x}}_{i,\mu|\mu}$ is $\hat{\mathsf{x}}_{i,0|0} = \begin{bmatrix} \bar{\vec{\mathsf{x}}}_0^T & 0^T \end{bmatrix}^T$. $K_{i,\mu+1}$ stands for the LF gain to be designed.

In the sequel, the corresponding prediction error and filtering error are expressed by $\tilde{\mathsf{x}}_{i,\mu+1|\mu} = \mathsf{x}_{\mu+1} - \hat{\mathsf{x}}_{i,\mu+1|\mu}$ and $\tilde{\mathsf{x}}_{i,\mu+1|\mu+1} = \mathsf{x}_{\mu+1} - \hat{\mathsf{x}}_{i,\mu+1|\mu+1}$. Firstly, by using (5) and (10), we obtain

$$\tilde{\mathsf{x}}_{i,\mu+1|\mu} = \tilde{A}_\mu \mathsf{x}_\mu + \bar{A}_\mu \tilde{\mathsf{x}}_{i,\mu|\mu} + f(\mathsf{x}_{\mu-d}) - f(\hat{\mathsf{x}}_{i,\mu-d|\mu-d}) + B_\mu w_\mu. \tag{12}$$

Then, by means of the Taylor series expansion of the function $f(\mathsf{x}_{\mu-d})$ regarding $\hat{\mathsf{x}}_{i,\mu-d|\mu-d}$, we have

$$f(\mathsf{x}_{\mu-d}) = f(\hat{\mathsf{x}}_{i,\mu-d|\mu-d}) + \mathsf{F}_{i,\mu-d}\tilde{\mathsf{x}}_{i,\mu-d|\mu-d} + o(|\tilde{\mathsf{x}}_{i,\mu-d|\mu-d}|), \tag{13}$$

where $\mathsf{F}_{i,\mu-d} = \partial f(\mathsf{x}_{\mu-d})/\partial \mathsf{x}_{\mu-d}|_{\mathsf{x}_{\mu-d}=\hat{\mathsf{x}}_{i,\mu-d|\mu-d}}$ and $o(|\tilde{\mathsf{x}}_{i,\mu-d|\mu-d}|)$ denotes the high-order term. In sequel, the term $o(|\tilde{\mathsf{x}}_{i,\mu-d|\mu-d}|)$ is approximated by $o(|\tilde{\mathsf{x}}_{i,\mu-d|\mu-d}|) = U_{i,\mu-d}\Lambda_{i,\mu-d}M_{i,\mu-d}\tilde{\mathsf{x}}_{i,\mu-d|\mu-d}$, where $U_{i,\mu-d}$ and $M_{i,\mu-d}$ are both known matrices, and $\Lambda_{i,\mu-d}$ is an unknown matrix, which is usually to depict the linearization error with $\Lambda_{i,\mu-d}\Lambda_{i,\mu-d}^T \preceq I$. Based on (13), equation (12) can be expressed as

$$\tilde{\mathsf{x}}_{i,\mu+1|\mu} = \tilde{A}_\mu \mathsf{x}_\mu + \bar{A}_\mu \tilde{\mathsf{x}}_{i,\mu|\mu} + (\mathsf{F}_{i,\mu-d} + U_{i,\mu-d}\Lambda_{i,\mu-d}M_{i,\mu-d})\tilde{\mathsf{x}}_{i,\mu-d|\mu-d} + B_\mu w_\mu. \tag{14}$$

Next, by subtracting (11) from (5), we obtain

$$\begin{aligned}\tilde{\mathsf{x}}_{i,\mu+1|\mu+1} &= \tilde{\mathsf{x}}_{i,\mu+1|\mu} - K_{i,\mu+1}(y_{i,\mu+1} - \bar{C}_{i,\mu+1}\hat{\mathsf{x}}_{i,\mu+1|\mu}) \\ &= (I - K_{i,\mu+1}\bar{C}_{i,\mu+1})\tilde{\mathsf{x}}_{i,\mu+1|\mu} - K_{i,\mu+1}\tilde{C}_{i,\mu+1}\mathsf{x}_{\mu+1} - \kappa_{\mu+1}^i K_{i,\mu+1}v_{i,\mu+1}.\end{aligned} \tag{15}$$

In the following, the corresponding PEC and FEC will be denoted by $\mathcal{T}_{i,\mu+1|\mu} = \mathbb{E}\{\tilde{\mathsf{x}}_{i,\mu+1|\mu}\tilde{\mathsf{x}}_{i,\mu+1|\mu}^T\}$ and $\mathcal{T}_{i,\mu+1|\mu+1} = \mathbb{E}\{\tilde{\mathsf{x}}_{i,\mu+1|\mu+1}\tilde{\mathsf{x}}_{i,\mu+1|\mu+1}^T\}$, respectively.

Our main purpose of this paper is to design the LF in the form of (10) and (11) such that, under the influences of the SCP and MFMs, the UB of each local FEC is derived and the obtained UB is locally minimized by means of taking appropriate filter gain at each moment. Furthermore, based on the LFs and UBs of the FEC, the distributed fusion filter $\hat{\mathsf{x}}_{\mu|\mu}^{ICI}$ and FEC $\Pi_{\mu|\mu}^{ICI}$ will be derived using the ICI fusion approach. Finally, a sufficient condition is provided for the developed DFF approach, under which the local UB is uniformly bounded.

3. Main Results

For each sensor subsystem, in this section, the local expressions with respect to FEC and PEC are presented, and then their UBs are capable of providing iterative form. Furthermore, by choosing a proper filter gain, the minimized UB of the FEC is obtained at each moment. On the basis of LFs, the fusion filter is computed by using the ICI fusion scheme.

3.1. Construction of the LF

To start, some Lemmas are provided, which will be utilized in the following derivations.

Lemma 1 *[48] For any $m_1, m_2 \in \mathbb{R}^n$, one has*

$$m_1 m_2^T + m_2 m_1^T \preceq \tau m_1 m_1^T + \tau^{-1} m_2 m_2^T,$$

where $\tau > 0$ is a scalar.

Lemma 2 *[49] Given matrices $\mathcal{Z}$, $\mathcal{X}$, C and $\mathcal{V}$ with suitable dimensions satisfying $\mathcal{V}\mathcal{V}^T \preceq I$, let matrix $Q \succ 0$ and $\pi > 0$ such that $\pi^{-1}I - CQC^T \succ 0$. Then, one has*

$$(\mathcal{Z} + \mathcal{X}\mathcal{V}C)Q(\mathcal{Z} + \mathcal{X}\mathcal{V}C)^T \preceq \mathcal{Z}(Q^{-1} - \pi C^T C)^{-1}\mathcal{Z}^T + \pi^{-1}\mathcal{X}\mathcal{X}^T.$$

Lemma 3 *[33] For a real matrix $A_{n\times n}$ and any random matrix $Y = \mathrm{diag}\{g_1, g_2, \cdots, g_n\}$, one has*

$$\mathbb{E}\{YAY^T\} = \begin{bmatrix} \mathbb{E}\{g_1^2\} & \mathbb{E}\{g_1 g_2\} & \cdots & \mathbb{E}\{g_1 g_n\} \\ \mathbb{E}\{g_2 g_1\} & \mathbb{E}\{g_2^2\} & \cdots & \mathbb{E}\{g_2 g_n\} \\ \vdots & \vdots & \ddots & \vdots \\ \mathbb{E}\{g_n g_1\} & \mathbb{E}\{g_n g_2\} & \cdots & \mathbb{E}\{g_n^2\} \end{bmatrix} \circ A,$$

where $\circ$ denotes the Hadamard product.

In view of the above preliminary preparation, the recursive formulations of the PEC and FEC are presented in the next derivations.

Theorem 1 *For sensor i ($i = 1, 2, \cdots, L$), the local PEC $\mathcal{T}_{i,\mu+1|\mu}$ and FEC $\mathcal{T}_{i,\mu+1|\mu+1}$ are characterized as*

$$\begin{aligned}\mathcal{T}_{i,\mu+1|\mu} &= \mathbb{E}\{\tilde{A}_\mu \mathsf{x}_\mu \mathsf{x}_\mu^T \tilde{A}_\mu^T\} + \bar{A}_\mu \mathcal{T}_{i,\mu|\mu} \bar{A}_\mu^T + (\mathsf{F}_{i,\mu-d} + U_{i,\mu-d}\Lambda_{i,\mu-d}M_{i,\mu-d})\mathcal{T}_{i,\mu-d|\mu-d} \\ &\quad \times(\mathsf{F}_{i,\mu-d} + U_{i,\mu-d}\Lambda_{i,\mu-d}M_{i,\mu-d})^T + O_i \circ (\breve{B}_\mu Q_\mu \breve{B}_\mu^T) + \mathcal{D}_{i,\mu} + \mathcal{D}_{i,\mu}^T, \qquad (16)\\ \mathcal{T}_{i,\mu+1|\mu+1} &= (I - K_{i,\mu+1}\bar{C}_{i,\mu+1})\mathcal{T}_{i,\mu+1|\mu}(I - K_{i,\mu+1}\bar{C}_{i,\mu+1})^T \\ &\quad + K_{i,\mu+1}\mathbb{E}\left\{\tilde{C}_{i,\mu+1}\mathsf{x}_{\mu+1}\mathsf{x}_{\mu+1}^T\tilde{C}_{i,\mu+1}^T\right\}K_{i,\mu+1}^T \\ &\quad + p_i K_{i,\mu+1} R_{i,\mu+1} K_{i,\mu+1}^T, \qquad (17)\end{aligned}$$

where

$$O_i = \begin{bmatrix} J_{n\times n} & p_i J_{n\times q_i} \\ p_i J_{q_i\times n} & p_i J_{q_i\times q_i}\end{bmatrix}, \quad J_{n\times m} = \begin{bmatrix} 1 & 1 & \dots & 1 \\ 1 & 1 & \dots & 1 \\ \vdots & \vdots & \ddots & \vdots \\ 1 & 1 & \dots & 1\end{bmatrix}_{n\times m},$$

$$\mathcal{D}_{i,\mu} = \bar{A}_\mu \mathbb{E}\{\tilde{\mathsf{x}}_{i,\mu|\mu}\tilde{\mathsf{x}}_{i,\mu-d|\mu-d}^T\}(\mathsf{F}_{i,\mu-d} + U_{i,\mu-d}\Lambda_{i,\mu-d}M_{i,\mu-d})^T.$$

Proof. *To begin with, based on (9) and (14) as well as the related definitions, we can easily obtain the conclusion that (16) is true.*

Next, by means of (15) and its covariance definition, we have

$$\begin{aligned}\mathcal{T}_{i,\mu+1|\mu+1} &= (I - K_{i,\mu+1}\bar{C}_{i,\mu+1})\mathcal{T}_{i,\mu+1|\mu}(I - K_{i,\mu+1}\bar{C}_{i,\mu+1})^T \\ &\quad + K_{i,\mu+1}\mathbb{E}\left\{\tilde{C}_{i,\mu+1}\mathsf{x}_{\mu+1}\mathsf{x}_{\mu+1}^T\tilde{C}_{i,\mu+1}^T\right\}K_{i,\mu+1}^T \\ &\quad + p_i K_{i,\mu+1} R_{i,\mu+1} K_{i,\mu+1}^T - \mathcal{E}_{i,\mu+1}^{(1)} - \mathcal{E}_{i,\mu+1}^{(1)T} \\ &\quad - \mathcal{E}_{i,\mu+1}^{(2)} - \mathcal{E}_{i,\mu+1}^{(2)T} + \mathcal{E}_{i,\mu+1}^{(3)} + \mathcal{E}_{i,\mu+1}^{(3)T},\end{aligned}$$

where

$$\begin{aligned}\mathcal{E}_{i,\mu+1}^{(1)} &= (I - K_{i,\mu+1}\bar{C}_{i,\mu+1})\mathbb{E}\left\{\tilde{\mathsf{x}}_{i,\mu+1|\mu}\mathsf{x}_{\mu+1}^T\tilde{C}_{i,\mu+1}^T\right\}K_{i,\mu+1}^T, \\ \mathcal{E}_{i,\mu+1}^{(2)} &= (I - K_{i,\mu+1}\bar{C}_{i,\mu+1})\mathbb{E}\left\{\tilde{\mathsf{x}}_{i,\mu+1|\mu}v_{i,\mu+1}^T\kappa_{\mu+1}^i\right\}K_{i,\mu+1}^T, \\ \mathcal{E}_{i,\mu+1}^{(3)} &= K_{i,\mu+1}\mathbb{E}\left\{\tilde{C}_{i,\mu+1}\mathsf{x}_{\mu+1}v_{i,\mu+1}^T\kappa_{\mu+1}^i\right\}K_{i,\mu+1}^T.\end{aligned}$$

It is obvious that $\mathcal{E}_{i,\mu+1}^{(s_1)} = 0$ ($s_1 = 1, 2, 3$), which yields (17). This completes the proof.

Remark 3 *On the basis of the previous Theorem 1, we can obtain the local covariances of the local prediction error and filtering error, respectively. Nevertheless, it is notable that the accurate FEC and PEC can not be directly derived due to the fact that the local covariance expressions (16) and (17) have some uncertain terms and cross terms. To overcome this issue, the corresponding UBs of local covariances are deduced, and then the LF gain is derived by minimizing the local UB with respect to the FEC.*

On the basis of the preceding discussions, the expressions of UB regarding FEC and PEC are represented in the recursive forms, which are shown in the following text.

Theorem 2 *For each sensor subsystem, let positive constants $\eta_{s_2} > 0$ ($s_2 = 1, 2, 3$) and $\varepsilon_{i,\mu-d} > 0$ be given. If the recursive difference equations:*

$$\begin{aligned}\Pi_{i,\mu+1|\mu} &= \lambda_{\max}(\bar{\Gamma}_{i,\mu}^1)\Gamma_{i,\mu}^2 + (1+\eta_2)\bar{A}_\mu \Pi_{i,\mu|\mu}\bar{A}_\mu^T + (1+\eta_2^{-1})\Big[\mathsf{F}_{i,\mu-d}(\Pi_{i,\mu-d|\mu-d}^{-1} \\ &\quad - \varepsilon_{i,\mu-d}M_{i,\mu-d}^T M_{i,\mu-d})^{-1}\mathsf{F}_{i,\mu-d}^T + \varepsilon_{i,\mu-d}^{-1}U_{i,\mu-d}U_{i,\mu-d}^T\Big] + O_i \circ (\breve{B}_\mu Q_\mu \breve{B}_\mu^T), \qquad (18)\\ \Pi_{i,\mu+1|\mu+1} &= (I - K_{i,\mu+1}\bar{C}_{i,\mu+1})\Pi_{i,\mu+1|\mu}(I - K_{i,\mu+1}\bar{C}_{i,\mu+1})^T + \lambda_{\max}(\bar{\Gamma}_{i,\mu+1}^3)K_{i,\mu+1}\Gamma_{i,\mu+1}^4 K_{i,\mu+1}^T \\ &\quad + p_i K_{i,\mu+1}R_{i,\mu+1}K_{i,\mu+1}^T, \qquad (19)\end{aligned}$$

under the initial condition $0 \prec \mathcal{T}_{i,-d|-d} \preceq \Pi_{i,-d|-d}$ $(d > 0)$ *and the following condition*

$$\varepsilon_{i,\mu-d}^{-1} I - M_{i,\mu-d} \Pi_{i,\mu-d|\mu-d} M_{i,\mu-d}^T \succ 0, \tag{20}$$

have solutions $\Pi_{i,\mu+1|\mu} \succ 0$ *and* $\Pi_{i,\mu+1|\mu+1} \succ 0$*, where*

$$\begin{aligned}
\bar{\Gamma}_{i,\mu}^1 &= (1+\eta_1)\Pi_{i,\mu|\mu} + (1+\eta_1^{-1})\hat{\mathsf{x}}_{i,\mu|\mu}\hat{\mathsf{x}}_{i,\mu|\mu}^T, \\
\breve{\Theta}_{i,\mu} &= \operatorname{diag}\left\{\rho_{i,\mu}^{(1)}, \rho_{i,\mu}^{(2)}, \cdots, \rho_{i,\mu}^{(q_i)}\right\}, \\
\vec{\Theta}_{i,\mu} &= \begin{bmatrix} (\bar{\theta}_{i,\mu}^{(1)})^2 + \rho_{i,\mu}^{(1)} & \bar{\theta}_{i,\mu}^{(1)}\bar{\theta}_{i,\mu}^{(2)} & \cdots & \bar{\theta}_{i,\mu}^{(1)}\bar{\theta}_{i,\mu}^{(q_i)} \\ * & (\bar{\theta}_{i,\mu}^{(2)})^2 + \rho_{i,\mu}^{(2)} & \cdots & \bar{\theta}_{i,\mu}^{(2)}\bar{\theta}_{i,\mu}^{(q_i)} \\ \vdots & \vdots & \ddots & \vdots \\ * & * & \cdots & (\bar{\theta}_{i,\mu}^{(q_1)})^2 + \rho_{i,\mu}^{(q_1)} \end{bmatrix}, \\
\Gamma_{i,\mu}^2 &= \operatorname{diag}\left\{0, \Gamma_{i,\mu}^4\right\}, \\
\bar{\Gamma}_{i,\mu+1}^3 &= (1+\eta_3)\Pi_{i,\mu+1|\mu} + (1+\eta_3^{-1})\hat{\mathsf{x}}_{i,\mu+1|\mu}\hat{\mathsf{x}}_{i,\mu+1|\mu}^T, \\
\Gamma_{i,\mu+1}^4 &= p_1(1-p_i)\vec{\Theta}_{i,\mu+1} \circ (\vec{C}_{i,\mu+1}\vec{C}_{i,\mu+1}^T) + p_i^2\breve{\Theta}_{i,\mu+1} \circ (\vec{C}_{i,\mu+1}\vec{C}_{i,\mu+1}^T) + p_i(1-p_i)I, \\
\Gamma_{i,\mu+1}^5 &= \bar{C}_{i,\mu+1}\Pi_{i,\mu+1|\mu}\bar{C}_{i,\mu+1}^T + \lambda_{\max}(\bar{\Gamma}_{i,\mu+1}^3)\Gamma_{i,\mu+1}^4 + p_i R_{i,\mu+1},
\end{aligned}$$

then it can be derived that

$$\mathcal{T}_{i,\mu+1|\mu+1} \preceq \Pi_{i,\mu+1|\mu+1}, \quad \mathcal{T}_{i,\mu+1|\mu} \preceq \Pi_{i,\mu+1|\mu}.$$

In addition, if the LF gain is designed as

$$K_{i,\mu+1} = \Pi_{i,\mu+1|\mu}\bar{C}_{i,\mu+1}^T(\Gamma_{i,\mu+1}^5)^{-1}, \tag{21}$$

then the minimal UB with regard to the FEC is derived at each time.

Proof. *According to previous results, this theorem can be proved via mathematical induction. It follows from the initial condition that we have* $0 \prec \mathcal{T}_{i,-d|-d} \preceq \Pi_{i,-d|-d}$*. Supposing* $\mathcal{T}_{i,\mu|\mu} \preceq \Pi_{i,\mu|\mu}$*, then we need to check* $\mathcal{T}_{i,\mu+1|\mu+1} \preceq \Pi_{i,\mu+1|\mu+1}$*. To begin with, the uncertain term of (16) can be tackled as*

$$\mathbb{E}\left\{\tilde{A}_\mu \mathsf{x}_\mu \mathsf{x}_\mu^T \tilde{A}_\mu^T\right\} \preceq \lambda_{\max}(\mathbb{E}\left\{\mathsf{x}_\mu \mathsf{x}_\mu^T\right\})\mathbb{E}\left\{\tilde{A}_\mu \tilde{A}_\mu^T\right\}. \tag{22}$$

According to Lemma 1, we have

$$\begin{aligned}
\mathbb{E}\left\{\mathsf{x}_\mu \mathsf{x}_\mu^T\right\} &= \mathbb{E}\left\{(\tilde{\mathsf{x}}_{i,\mu|\mu} + \hat{\mathsf{x}}_{i,\mu|\mu})(\tilde{\mathsf{x}}_{i,\mu|\mu} + \hat{\mathsf{x}}_{i,\mu|\mu})^T\right\} \\
&\preceq (1+\eta_1)\mathcal{T}_{i,\mu|\mu} + (1+\eta_1^{-1})\hat{\mathsf{x}}_{i,\mu|\mu}\hat{\mathsf{x}}_{i,\mu|\mu}^T \\
&:= \Gamma_{i,\mu}^1,
\end{aligned} \tag{23}$$

where $\eta_1 > 0$ *is a scalar. It follows from (7) and Lemma 3 that*

$$\begin{aligned}
\mathbb{E}\left\{\tilde{A}_\mu \tilde{A}_\mu^T\right\} &= \operatorname{diag}\left\{0, p_1(1-p_i)\vec{\Theta}_{i,\mu} \circ (\vec{C}_{i,\mu}\vec{C}_{i,\mu}^T) + p_i^2\breve{\Theta}_{i,\mu} \circ (\vec{C}_{i,\mu}\vec{C}_{i,\mu}^T) + p_i(1-p_i)I\right\} \\
&:= \Gamma_{i,\mu}^2,
\end{aligned} \tag{24}$$

where $\breve{\Theta}_{i,\mu}$ *and* $\vec{\Theta}_{i,\mu}$ *are presented below (20). Substituting (23) and (24) into (22), we have*

$$\mathbb{E}\left\{\tilde{A}_\mu \mathsf{x}_\mu \mathsf{x}_\mu^T \tilde{A}_\mu^T\right\} \preceq \lambda_{\max}(\Gamma_{i,\mu}^1)\Gamma_{i,\mu}^2. \tag{25}$$

Next, according to Lemma 1, the cross term of (16) is represented by:

$$\begin{aligned}
\mathcal{D}_{i,\mu} + \mathcal{D}_{i,\mu}^T \preceq\ & \eta_2 \bar{A}_\mu \mathcal{T}_{i,\mu|\mu}\bar{A}_\mu^T + \eta_2^{-1}(\mathsf{F}_{i,\mu-d} + U_{i,\mu-d}\Lambda_{i,\mu-d}M_{i,\mu-d})\mathcal{T}_{i,\mu-d|\mu-d} \\
& \times(\mathsf{F}_{i,\mu-d} + U_{i,\mu-d}\Lambda_{i,\mu-d}M_{i,\mu-d})^T,
\end{aligned} \tag{26}$$

where $\eta_2 > 0$ is a scalar. By means of Lemma 2 and (20), we have

$$\begin{aligned}&(\mathsf{F}_{i,\mu-d} + U_{i,\mu-d}\Lambda_{i,\mu-d}M_{i,\mu-d})\mathcal{T}_{i,\mu-d|\mu-d}(\mathsf{F}_{i,\mu-d} + U_{i,\mu-d}\Lambda_{i,\mu-d}M_{i,\mu-d})^T\\ \leq\ & \mathsf{F}_{i,\mu-d}(\Pi^{-1}_{i,\mu-d|\mu-d} - \varepsilon_{i,\mu-d}M^T_{i,\mu-d}M_{i,\mu-d})^{-1}\mathsf{F}^T_{i,\mu-d} + \varepsilon^{-1}_{i,\mu-d}U_{i,\mu-d}U^T_{i,\mu-d},\end{aligned} \tag{27}$$

where $\varepsilon_{i,\mu-d} > 0$ is a scalar. By using (25)-(27), we can deduce that

$$\begin{aligned}\mathcal{T}_{i,\mu+1|\mu} \leq\ & \lambda_{\max}(\bar{\Gamma}^1_{i,\mu})\Gamma^2_{i,\mu} + (1+\eta_2)\bar{A}_\mu\Pi_{i,\mu|\mu}\bar{A}^T_\mu + (1+\eta_2^{-1})\\ & \times\left[\mathsf{F}_{i,\mu-d}(\Pi^{-1}_{i,\mu-d|\mu-d} - \varepsilon_{i,\mu-d}M^T_{i,\mu-d}M_{i,\mu-d})^{-1}\mathsf{F}^T_{i,\mu-d} + \varepsilon^{-1}_{i,\mu-d}U_{i,\mu-d}U^T_{i,\mu-d}\right]\\ & + O_i \circ (\breve{B}_\mu Q_\mu \breve{B}^T_\mu).\end{aligned} \tag{28}$$

Subsequently, it will be deduced that $\mathcal{T}_{i,\mu+1|\mu+1} \leq \Pi_{i,\mu+1|\mu+1}$. The uncertain term of (17) can be tackled by:

$$\mathbb{E}\left\{\tilde{C}_{i,\mu+1}\mathsf{x}_{\mu+1}\mathsf{x}^T_{\mu+1}\tilde{C}^T_{i,\mu+1}\right\} \leq \lambda_{\max}(\mathbb{E}\left\{\mathsf{x}_{\mu+1}\mathsf{x}^T_{\mu+1}\right\})\mathbb{E}\left\{\tilde{C}_{i,\mu+1}\tilde{C}^T_{i,\mu+1}\right\}. \tag{29}$$

Recalling Lemma 1, we have

$$\begin{aligned}\mathbb{E}\left\{\mathsf{x}_{\mu+1}\mathsf{x}^T_{\mu+1}\right\} &= \mathbb{E}\left\{(\tilde{\mathsf{x}}_{i,\mu+1|\mu} + \hat{\mathsf{x}}_{i,\mu+1|\mu})(\tilde{\mathsf{x}}_{i,\mu+1|\mu} + \hat{\mathsf{x}}_{i,\mu+1|\mu})^T\right\}\\ &\leq (1+\eta_3)\mathcal{T}_{i,\mu+1|\mu} + (1+\eta_3^{-1})\hat{\mathsf{x}}_{i,\mu+1|\mu}\hat{\mathsf{x}}^T_{i,\mu+1|\mu}\\ &:= \Gamma^3_{i,\mu+1},\end{aligned} \tag{30}$$

where $\eta_3 > 0$ is a scalar. According to (8) and Lemma 3, we can obtain

$$\begin{aligned}\mathbb{E}\left\{\tilde{C}_{i,\mu+1}\tilde{C}^T_{i,\mu+1}\right\} &= p_1(1-p_i)\vec{\Theta}_{i,\mu+1} \circ (\vec{C}_{i,\mu+1}\vec{C}^T_{i,\mu+1}) + p_i^2\breve{\Theta}_{i,\mu+1} \circ (\vec{C}_{i,\mu+1}\vec{C}^T_{i,\mu+1}) + p_i(1-p_i)I\\ &:= \Gamma^4_{i,\mu+1}.\end{aligned} \tag{31}$$

Substituting (30) and (31) into (29), we have

$$\mathbb{E}\left\{\tilde{C}_{i,\mu+1}\mathsf{x}_{\mu+1}\mathsf{x}^T_{\mu+1}\tilde{C}^T_{i,\mu+1}\right\} \leq \lambda_{\max}(\Gamma^3_{i,\mu+1})\Gamma^4_{i,\mu+1}. \tag{32}$$

Substituting (32) into (17) yields

$$\begin{aligned}\mathcal{T}_{i,\mu+1|\mu+1} \leq\ & (I - K_{i,\mu+1}\bar{C}_{i,\mu+1})\mathcal{T}_{i,\mu+1|\mu}(I - K_{i,\mu+1}\bar{C}_{i,\mu+1})^T + \lambda_{\max}(\Gamma^3_{i,\mu+1})K_{i,\mu+1}\Gamma^4_{i,\mu+1}K^T_{i,\mu+1}\\ & + p_iK_{i,\mu+1}R_{i,\mu+1}K^T_{i,\mu+1}.\end{aligned} \tag{33}$$

On the basis of the induction method as well as (18), (19), (28) and (33), we have

$$\begin{aligned}\mathcal{T}_{i,\mu+1|\mu+1} \leq\ & (I - K_{i,\mu+1}\bar{C}_{i,\mu+1})\Pi_{i,\mu+1|\mu}(I - K_{i,\mu+1}\bar{C}_{i,\mu+1})^T + \lambda_{\max}(\bar{\Gamma}^3_{i,\mu+1})K_{i,\mu+1}\Gamma^4_{i,\mu+1}K^T_{i,\mu+1}\\ & + p_iK_{i,\mu+1}R_{i,\mu+1}K^T_{i,\mu+1},\end{aligned}$$

where $\bar{\Gamma}^3_{i,\mu+1}$ is given below (20). As such, we conclude that $\mathcal{T}_{i,\mu+1|\mu+1} \leq \Pi_{i,\mu+1|\mu+1}$ is true.

Finally, in order to deduce the optimized UB of the FEC, the partial derivative of $\mathrm{tr}(\Pi_{i,\mu+1|\mu+1})$ *regarding the filter gain is computed by:*

$$\begin{aligned}\frac{\partial \mathrm{tr}(\Pi_{i,\mu+1|\mu+1})}{\partial K_{i,\mu+1}} &= -2(I - K_{i,\mu+1}\bar{C}_{i,\mu+1})\Pi_{i,\mu+1|\mu}\bar{C}^T_{i,\mu+1} + 2\lambda_{\max}(\bar{\Gamma}^3_{i,\mu+1})K_{i,\mu+1}\Gamma^4_{i,\mu+1}\\ &\quad + 2p_iK_{i,\mu+1}R_{i,\mu+1}.\end{aligned} \tag{34}$$

Then, letting the above result be zero, it is easy to see that (21) is true, which completes the proof.

In the light of the Theorem 2, the local UB on the FEC can be obtained and then locally minimized by using the proper filter gain for each processor at each moment. Based on the LFs from all processors, next, the fusion filter and its covariance is presented by exploiting the ICI fusion method.

3.2. Fusion Filtering Approach

Based on the fact that SCP is used in the MSNSs, the expressions of the cross-covariance between any two local filtering errors are hard to obtain. Therefore, the WM fusion method, which requires the cross-covariance with respect to filtering error and prediction error, is not applicable to handle the DFF problem. In the following text, the DFF algorithm is realized based on ICI fusion rule by only using the local FEC [14].

In this subsection, with the help of LF $\hat{\mathrm{x}}_{i,\mu|\mu}$ $(i = 1, \cdots, L)$ and its UB on the FEC $\Pi_{i,\mu|\mu}$, the ICI fusion filter $\hat{\mathrm{x}}^{ICI}_{\mu|\mu}$ and covariance $\Pi^{ICI}_{\mu|\mu}$ are given as

$$\hat{\mathrm{x}}^{ICI}_{\mu|\mu} = \sum_{i=1}^{L} \Upsilon^{ICI}_{i,\mu|\mu} \hat{\mathrm{x}}_{i,\mu|\mu}, \tag{35}$$

$$\Pi^{ICI}_{\mu|\mu} = \left[\sum_{i=1}^{L} \Pi^{-1}_{i,\mu|\mu} - \left(\sum_{i=1}^{L} n_i \Pi_{i,\mu|\mu} \right)^{-1} \right]^{-1}, \tag{36}$$

where $0 \leq n_i \leq 1$ is a weighting coefficient meeting $\sum_{i=1}^{L} n_i = 1$. The fusion gains $\Upsilon^{ICI}_{i,\mu|\mu}$ are obtained by:

$$\Upsilon^{ICI}_{i,\mu|\mu} = \Pi^{ICI}_{\mu|\mu} \left[\Pi^{-1}_{i,\mu|\mu} - n_i \left(\sum_{i=1}^{L} n_i \Pi_{i,\mu|\mu} \right)^{-1} \right]. \tag{37}$$

The DFF algorithm can be carried out by solving the following optimization problem:

$$\begin{aligned} &\min_{n_i} \left\{ \mathrm{tr}(\Pi^{ICI}_{\mu|\mu}) \right\}, \\ \text{s.t.} \quad &\sum_{i=1}^{L} n_i = 1, \quad n_i \in [0,\ 1]. \end{aligned} \tag{38}$$

The solution of (38) can be calculated in terms of the "fmincon" function in Matlab.

In terms of above results and literature [14], we can easily derive that $\Pi^{ICI}_{\mu|\mu} \leq \Pi_{i,\mu|\mu}$. In addition, compared with the CI fusion rule, the ICI fusion rule is a generally lesser conservative fusion rule, which can more accurately estimate the fusion covariance matrix based on the FECs from different sensors and automatically adjust the weights by means of the optimization toolbox, thereby improving the accuracy of the fusion results. In what follows, according to the recursive formulations regarding local UBs in Theorem 2 and the ICI fusion method, the SCP-based DFF (SCPBDFF) algorithm can be given (see Table 1).

Table 1. Steps of SCPBDFF algorithm.

Algorithm 1 SCPBDFF Algorithm
$Step\ 1$: Let $\mu = 0$ and choose the initial values.
$Step\ 2$: Compute the prediction $\hat{\mathrm{x}}_{i,\mu+1|\mu}$ based on (10).
$Step\ 3$: Calculate the PEC $\Pi_{i,\mu+1|\mu}$ by means of (18).
$Step\ 4$: Derive the gain matrix $K_{i,\mu+1}$ according to (21).
$Step\ 5$: Calculate $\hat{\mathrm{x}}_{i,\mu+1|\mu+1}$ according to (11).
$Step\ 6$: Compute the UB of the FEC $\Pi_{i,\mu+1|\mu+1}$ based on (19).
$Step\ 7$: Get the fusion estimation $\hat{\mathrm{x}}^{ICI}_{\mu|\mu}$ and EEC $\Pi^{ICI}_{\mu|\mu}$ by (35) as well as (36), respectively.
$Step\ 8$: Set $\mu = \mu + 1$, and return to $Step\ 2$.

Remark 4 *Based on the above text, the new SCPBDFF algorithm has been summarized for the tackled system with multiple sensors, and each step of the algorithm can be realized by using the related recursive expressions. In this regard, the corresponding local results (e.g., LF, LF gain, UBs regarding FEC and PEC) are shown in (10), (11), (21), (18), and (19). As the iteration number increases, the fusion filter $\hat{\mathrm{x}}^{ICI}_{\mu|\mu}$ and its covariance $\Pi^{ICI}_{\mu|\mu}$ in (35) and (36) can be obtained. Therefore, the developed SCPBDFF approach is capable of using online and real-time processing. Moreover, the algorithm has the characteristic of parallel processing, and its efficiency can be further improved.*

4. Boundedness Analysis

Combined with theory and application, the boundedness of the FEC that reflects the estimation performance is desirable. In this section, in order to guarantee the boundedness of UB on FEC, a sufficient condition is presented. Subsequently, the assumption and theorem are provided as follows.

Assumption 1 *There exist positive real numbers $\bar{a}$, $\bar{b}$, $\bar{c}$, $\bar{\mathsf{f}}$, $\bar{m}$, $\bar{u}$, $\underline{r}$, $\vec{\theta}$, $\bar{o}$, $\bar{r}$, $\bar{q}$, $\bar{\theta}$, $\bar{\rho}$, and $\bar{\mathsf{x}}$ such that*

$$\begin{aligned}
\bar{A}_\mu\bar{A}_\mu^T &\preceq \bar{a}I,\ \breve{B}_\mu\breve{B}_\mu^T \preceq \bar{b}I,\ \vec{C}_{i,\mu}\vec{C}_{i,\mu}^T \preceq \bar{c}I,\\
\mathsf{F}_{i,\mu-d}\mathsf{F}_{i,\mu-d}^T &\preceq \bar{\mathsf{f}}I,\ M_{i,\mu-d}M_{i,\mu-d}^T \preceq \bar{m}I,\ U_{i,\mu-d}U_{i,\mu-d}^T \preceq \bar{u}I,\\
\underline{r}I &\preceq R_{i,\mu} \preceq \bar{r}I,\ Q_\mu \preceq \bar{q}I,\ \bar{\Theta}_{i,\mu} \preceq \bar{\theta}I,\ \breve{\Theta}_{i,\mu} \preceq \bar{\rho}I,\\
\vec{\Theta}_{i,\mu} &\preceq \vec{\theta}I,\ p_i \le 1,\ O_i \preceq \bar{o}I,\ \hat{\mathsf{x}}_{i,\mu|\mu}\hat{\mathsf{x}}_{i,\mu|\mu}^T \preceq \bar{\mathsf{x}}I.
\end{aligned}$$

In addition, the following notations are presented:

$$\begin{aligned}
\tilde{\mathsf{x}} &\triangleq (1+\eta_4)\bar{\mathsf{x}}\bar{a} + (1+\eta_4^{-1})\left[(\bar{\mathsf{x}}^{-1} - \alpha\bar{m})^{-1}\bar{\mathsf{f}} + \alpha^{-1}\bar{u}\right],\\
\bar{k} &\triangleq \frac{\tilde{\psi}^2(\bar{\theta}^2\bar{c}+1)}{\underline{r}^2},\\
\tilde{\psi} &\triangleq \left[(1+\eta_1)\bar{\psi} + (1+\eta_1^{-1})\bar{\mathsf{x}}\right](\vec{\theta}\bar{c} + \bar{\rho}\bar{c} + 1) + (1+\eta_2)\bar{\psi}\bar{a}\\
&\quad +(1+\eta_2^{-1})\left[(\bar{\psi}^{-1} - \varepsilon\bar{m})^{-1}\bar{\mathsf{f}} + \varepsilon^{-1}\bar{u}\right] + \bar{o}\bar{b}\bar{q},\\
\beta &\triangleq 2\tilde{\psi}\left[1 + \bar{k}(\bar{\theta}^2\bar{c}+1)\right] + \left[(1+\eta_3)\tilde{\psi} + (1+\eta_3^{-1})\bar{\mathsf{x}}\right](\vec{\theta}\bar{c} + \bar{\rho}\bar{c} + 1)\bar{k} + \bar{r}\bar{k},
\end{aligned} \tag{39}$$

where $\bar{\psi}$ is a positive scalar. Moreover, the relevant scalars $\alpha_{i,\mu-d} = \alpha$, $\varepsilon_{i,\mu-d} = \varepsilon$, and $\eta_{s_3}(s_3 = 1,2,3,4)$ are set as fixed values.

In the light of Assumption 1, the following theorem is given, which can ensure that the filtering error is uniformly bounded in the mean-square case.

Theorem 3 *Under the Assumption 1 and notations (39), if the constraint conditions $\bar{m}\bar{\psi} < \varepsilon^{-1}$, $\bar{m}\bar{\mathsf{x}} < \alpha^{-1}$, and $\beta \le \bar{\psi}$ are satisfied with the initial condition $\Pi_{i,-d|-d} \preceq \bar{\psi}I$ $(d > 0)$, then $\Pi_{i,\mu|\mu} \preceq \bar{\psi}I$ holds for any μ.*

Proof. *According to the mathematical induction, this Theorem will be proven. To begin, based on the initial condition, we have $\Pi_{i,-d|-d} \preceq \bar{\psi}I$. Next, assuming $\Pi_{i,\mu|\mu} \preceq \bar{\psi}I$, we will check that $\Pi_{i,\mu+1|\mu+1} \preceq \bar{\psi}I$. Noticing the term $\bar{\Gamma}_{i,\mu}^1$ of (18), we have*

$$\begin{aligned}
\bar{\Gamma}_{i,\mu}^1 &= (1+\eta_1)\Pi_{i,\mu|\mu} + (1+\eta_1^{-1})\hat{\mathsf{x}}_{i,\mu|\mu}\hat{\mathsf{x}}_{i,\mu|\mu}^T\\
&\preceq \left[(1+\eta_1)\bar{\psi} + (1+\eta_1^{-1})\bar{\mathsf{x}}\right]I.
\end{aligned} \tag{40}$$

Based on the condition $\bar{m}\bar{\psi} < \varepsilon^{-1}$ and Lemma 2, we obtain

$$(\Pi_{i,\mu-d|\mu-d}^{-1} - \varepsilon M_{i,\mu-d}^T M_{i,\mu-d})^{-1} \preceq (\bar{\psi}^{-1} - \varepsilon\bar{m})^{-1}I. \tag{41}$$

It follows from (40) and (41) that

$$\begin{aligned}
\Pi_{i,\mu+1|\mu} &\preceq \left[(1+\eta_1)\bar{\psi} + (1+\eta_1^{-1})\bar{\mathsf{x}}\right]\Gamma_{i,\mu}^2 + (1+\eta_2)\bar{\psi}\bar{A}_\mu\bar{A}_\mu^T\\
&\quad +(1+\eta_2^{-1})\left[(\bar{\psi}^{-1} - \varepsilon\bar{m})^{-1}\mathsf{F}_{i,\mu-d}\mathsf{F}_{i,\mu-d}^T + \varepsilon^{-1}U_{i,\mu-d}U_{i,\mu-d}^T\right] + O_i \circ (\breve{B}_\mu Q_\mu \breve{B}_\mu^T).
\end{aligned} \tag{42}$$

Furthermore, the term $\Gamma_{i,\mu}^2$ of (42) can be rewritten as follows:

$$\begin{aligned}
\Gamma_{i,\mu}^2 &\preceq \Gamma_{i,\mu}^4 I\\
&= p_1(1-p_i)\vec{\Theta}_{i,\mu+1} \circ (\vec{C}_{i,\mu+1}\vec{C}_{i,\mu+1}^T) + p_i^2\breve{\Theta}_{i,\mu+1} \circ (\vec{C}_{i,\mu+1}\vec{C}_{i,\mu+1}^T) + p_i(1-p_i)I\\
&\preceq (\vec{\theta}\bar{c} + \bar{\rho}\bar{c} + 1)I.
\end{aligned} \tag{43}$$

In the light of (43) and Assumption 1, we have

$$\begin{aligned}\Pi_{i,\mu+1|\mu} &\leq \{\Big[(1+\eta_1)\bar{\psi}+(1+\eta_1^{-1})\bar{\mathsf{x}}\Big](\vec{\theta}\bar{c}+\bar{\rho}\bar{c}+1)+(1+\eta_2)\bar{\psi}\bar{a}\\ &\quad+(1+\eta_2^{-1})\Big[(\bar{\psi}^{-1}-\varepsilon\bar{m})^{-1}\bar{\mathsf{f}}+\varepsilon^{-1}\bar{u}\Big]+\bar{o}\bar{b}\bar{q}\}I\\ &= \tilde{\psi}I. \end{aligned} \tag{44}$$

On the basis of (10) and (13) as well as the condition $f(\mathsf{x}_{\mu-d})|_{\mathsf{x}_{\mu-d}=0}=0$, we have

$$\hat{\mathsf{x}}_{i,\mu+1|\mu}=\bar{A}_\mu\hat{\mathsf{x}}_{i,\mu|\mu}+(\mathsf{F}_{i,\mu-d}+U_{i,\mu-d}\Lambda_{i,\mu-d}M_{i,\mu-d})\hat{\mathsf{x}}_{i,\mu-d|\mu-d}. \tag{45}$$

It follows from (45) that

$$\begin{aligned}\hat{\mathsf{x}}_{i,\mu+1|\mu}\hat{\mathsf{x}}_{i,\mu+1|\mu}^T &\leq (1+\eta_4)\bar{A}_\mu\hat{\mathsf{x}}_{i,\mu|\mu}\hat{\mathsf{x}}_{i,\mu|\mu}^T\bar{A}_\mu^T+(1+\eta_4^{-1})(\mathsf{F}_{i,\mu-d}+U_{i,\mu-d}\Lambda_{i,\mu-d}M_{i,\mu-d})\hat{\mathsf{x}}_{i,\mu-d|\mu-d}\\ &\quad\times\hat{\mathsf{x}}_{i,\mu-d|\mu-d}^T(\mathsf{F}_{i,\mu-d}+U_{i,\mu-d}\Lambda_{i,\mu-d}M_{i,\mu-d})^T,\end{aligned}$$

where $\eta_4>0$ is a scalar. According to the condition $\bar{m}\bar{\mathsf{x}}<\alpha^{-1}$, we can easily have

$$\alpha^{-1}I-M_{i,\mu-d}\hat{\mathsf{x}}_{i,\mu-d|\mu-d}\hat{\mathsf{x}}_{i,\mu-d|\mu-d}^TM_{i,\mu-d}^T\succ 0.$$

Next, it follows from Lemma 2 that

$$\begin{aligned}\hat{\mathsf{x}}_{i,\mu+1|\mu}\hat{\mathsf{x}}_{i,\mu+1|\mu}^T &\leq (1+\eta_4)\bar{\mathsf{x}}\bar{A}_\mu\bar{A}_\mu^T+(1+\eta_4^{-1})\Big\{\mathsf{F}_{i,\mu-d}[(\hat{\mathsf{x}}_{i,\mu-d|\mu-d}\hat{\mathsf{x}}_{i,\mu-d|\mu-d}^T)^{-1}\\ &\quad-\alpha M_{i,\mu-d}^TM_{i,\mu-d}]^{-1}\mathsf{F}_{i,\mu-d}^T+\alpha^{-1}U_{i,\mu-d}U_{i,\mu-d}^T\Big\}\\ &\leq \Big\{(1+\eta_4)\bar{\mathsf{x}}\bar{a}+(1+\eta_4^{-1})\Big[(\bar{\mathsf{x}}^{-1}-\alpha\bar{m})^{-1}\bar{\mathsf{f}}+\alpha^{-1}\bar{u}\Big]\Big\}I\\ &= \tilde{\mathsf{x}}I.\end{aligned} \tag{46}$$

Moreover, it follows from the term $(\Gamma_{i,\mu+1}^5)^{-1}$ of (21) that

$$(\Gamma_{i,\mu+1}^5)^{-1}\leq\frac{1}{\underline{r}}I. \tag{47}$$

Then, from (21) and (47) , we have

$$\begin{aligned}K_{i,\mu+1}K_{i,\mu+1}^T &= \Pi_{i,\mu+1|\mu}\bar{C}_{i,\mu+1}^T(\Gamma_{i,\mu+1}^5)^{-1}(\Gamma_{i,\mu+1}^5)^{-1}\bar{C}_{i,\mu+1}\Pi_{i,\mu+1|\mu}\\ &\leq \frac{\tilde{\psi}^2(\bar{\theta}^2\bar{c}+1)}{\underline{r}^2}I\\ &= \bar{k}I.\end{aligned} \tag{48}$$

In the light of (44), (46), and (48) as well as Assumption 1, we have

$$\begin{aligned}\Pi_{i,\mu+1|\mu+1} &\leq \tilde{\psi}(I-K_{i,\mu+1}\bar{C}_{i,\mu+1})(I-K_{i,\mu+1}\bar{C}_{i,\mu+1})^T+\Big[(1+\eta_3)\tilde{\psi}+(1+\eta_3^{-1})\tilde{\mathsf{x}}\Big](\vec{\theta}\bar{c}+\bar{\rho}\bar{c}+1)K_{i,\mu+1}K_{i,\mu+1}^T\\ &\quad+\bar{r}K_{i,\mu+1}K_{i,\mu+1}^T\\ &\leq \Big\{2\tilde{\psi}\Big[1+\bar{k}(\bar{\theta}^2\bar{c}+1)\Big]+\Big[(1+\eta_3)\tilde{\psi}+(1+\eta_3^{-1})\tilde{\mathsf{x}}\Big](\vec{\theta}\bar{c}+\bar{\rho}\bar{c}+1)\bar{k}+\bar{r}\bar{k}\Big\}I\\ &= \beta I.\end{aligned}$$

Then, according to the condition $\beta\leq\bar{\psi}$, we derive that $\Pi_{i,\mu+1|\mu+1}\leq\bar{\psi}I$. Therefore, this completes the proof.

Remark 5 *It is easy to deduce that $\mathbb{E}\{\vec{\tilde{\mathsf{x}}}_{i,\mu|\mu}\vec{\tilde{\mathsf{x}}}_{i,\mu|\mu}^T\}=[I\ \ 0]\mathbb{E}\{\tilde{\mathsf{x}}_{i,\mu|\mu}\tilde{\mathsf{x}}_{i,\mu|\mu}^T\}[I\ \ 0]^T\leq[I\ \ 0]\Pi_{i,\mu|\mu}[I\ \ 0]^T\leq\bar{\psi}I$. In the light of the Schur complement Lemma, we derive $\mathbb{E}\{\|\vec{\tilde{\mathsf{x}}}_{i,\mu|\mu}\|^2\}\leq\bar{\psi}$. Hence, it can be checked that the filtering error is uniform bounded in mean-square case.*

Remark 6 *By means of the above theoretic analyses, we have presented a new SCPBDFF approach for nonlinear delayed MSNSs in the presence of MFMs and SCP. It is obvious to know that main results clearly manifest the impacts of MFMs and SCP on the DFF algorithm design. Specifically, $\Theta_{i,\mu}$ describes the phenomenon of the MFMs, and $\{\kappa_\mu\}_{\mu>0}$ reflects the determined sensor node when the measurement information is transferred on the network at each moment. Moreover, it is worth noting that the positive scalars $\varepsilon_{i,\mu-d} > 0$ $(i = 1, 2, \cdots, L)$ are introduced when dealing with the high-order terms of the Taylor series expansions. In order to obtain the minimized UB on FEC, we can adjust the values of $\varepsilon_{i,\mu-d} > 0$ to guarantee the feasibility of the constraint condition (20), which can further improve the flexibility of the proposed algorithm and provide different UB on FEC accordingly. Furthermore, the additional effort has been done to discuss the performance of the SCPBDFF algorithm, and then the uniform boundedness of the UB with regard to the FEC can be ensured by means of a sufficient condition in Theorem 3. In addition, when the state evolution function and observation function are both nonlinear and the nonlinear functions have the characteristics of the continuous differentiability, the similar main results can be obtained.*

5. Two Simulation Examples

In what follows, we will use two simulation examples to examine the validity of the proposed DFF method.

5.1. Example 1

Consider a discrete time-varying nonlinear three-sensor system (1) and (2) with related parameters given as follows:

$$\begin{aligned}
\vec{A}_\mu &= \begin{bmatrix} 0.265 & 0.134 \\ -0.15 & 0.195 \end{bmatrix}, \quad \vec{B}_\mu = \begin{bmatrix} -0.068 + 0.1\cos(0.1\mu) \\ -0.067 + 0.1\cos(0.2\mu) \end{bmatrix}, \\
\vec{C}_{1,\mu} &= \begin{bmatrix} 1.91 + 0.1\cos(0.1\mu) & 1.491 + 0.1\cos(0.1\mu) \end{bmatrix}, \\
\vec{C}_{2,\mu} &= \begin{bmatrix} 1.9 + 0.1\sin(0.1\mu) & 1.98 + 0.1\sin(0.1\mu) \end{bmatrix}, \\
\vec{C}_{3,\mu} &= \begin{bmatrix} 1.9 + 0.2\cos(0.2\mu) & 1.69 + 0.2\cos(0.2\mu) \end{bmatrix}.
\end{aligned}$$

The nonlinear function $\vec{f}(\vec{\mathrm{x}}_{\mu-d})$ with time-delay is given by:

$$\vec{f}(\vec{\mathrm{x}}_{\mu-d}) = \begin{bmatrix} 0.146\vec{\mathrm{x}}^1_{\mu-d} - 0.41\vec{\mathrm{x}}^2_{\mu-d} + 0.1\sin(\mu)\vec{\mathrm{x}}^1_{\mu-d}\vec{\mathrm{x}}^2_{\mu-d} \\ -0.195\vec{\mathrm{x}}^1_{\mu-d} + 0.2232\vec{\mathrm{x}}^2_{\mu-d} + 0.2\sin(\mu)\vec{\mathrm{x}}^1_{\mu-d}\vec{\mathrm{x}}^2_{\mu-d} \end{bmatrix}.$$

where $\vec{\mathrm{x}}_{\mu-d} = \begin{bmatrix} \vec{\mathrm{x}}^1_{\mu-d} & \vec{\mathrm{x}}^2_{\mu-d} \end{bmatrix}^T$ is system state.

In this example, select parameters as $\eta_1 = \eta_3 = 0.04, \eta_2 = 0.01$, $U_{i,\mu-d} = 0.01I$, $M_{i,\mu-d} = 0.01I$, $\varepsilon_{i,\mu-d} = [1.5\lambda_{\max}(M_{i,\mu-d}\Pi_{i,\mu-d|\mu-d}M^T_{i,\mu-d}) + 1]^{-1}$, and the time-delay is selected as $d = 1$. $\vec{w}_\mu$ and $\vec{v}_{i,\mu}$ $(i = 1, 2, 3)$ are zero-mean noises and their variances are $\vec{Q}_\mu = 0.059$, $R_{1,\mu} = 0.3$, $R_{2,\mu} = 0.34$ and $R_{3,\mu} = 0.35$, respectively. Besides, let $\Theta_{i,\mu} = \mathrm{diag}\left\{\theta^{(1)}_{i,\mu}\right\}$ $(i = 1, 2, 3)$, where the probability mass function for $\theta^{(1)}_{i,\mu}$ satisfies

$$\mathrm{Prob}\{\theta^{(1)}_{i,\mu} = s\} = \begin{cases} 0.2, & s = 0, \\ 0.4, & s = 0.4, \\ 0.4, & s = 1, \end{cases}$$

so their expectations and variances are easily derived as $\bar{\theta}^{(1)}_{i,\mu} = 0.56$ and $\rho^{(1)}_{i,\mu} = 0.1504$, respectively. The initial values are set as $\bar{\vec{\mathrm{x}}}_{-1} = \bar{\vec{\mathrm{x}}}_0 = \begin{bmatrix} 1 & -2.2 \end{bmatrix}^T$, $\hat{\mathrm{x}}_{i,-1|-1} = \hat{\mathrm{x}}_{i,0|0} = \begin{bmatrix} \bar{\vec{\mathrm{x}}}^T_0 & 0^T \end{bmatrix}^T$, $\vec{P}_{-1|-1} = \vec{P}_{0|0} = 2.5I$, $\Pi_{i,-1|-1} = \Pi_{i,0|0} = 2.5I$. Next, for SCP, the probabilities of each sensor to be selected are given as $\mathrm{Prob}\left\{\kappa_\mu = 1\right\} = 0.3$, $\mathrm{Prob}\left\{\kappa_\mu = 2\right\} = 0.4$ and $\mathrm{Prob}\left\{\kappa_\mu = 3\right\} = 0.3$. The accumulated MSE stands for an accuracy index for the filtering of the state $\vec{\mathrm{x}}_\mu$, which is defined as $\Sigma^\mu_{k=1}\left(\Sigma^{100}_{\iota=1}(\vec{\mathrm{x}}^\iota_{j,k} - \hat{x}^\iota_{j,i,k|k})^2\right)/100$ $(j = 1, 2)$. Here, the j stands for the jth state component and ι is the ιth simulation experiment.

Subsequently, the SCPBDFF algorithm is carried out and the related results are displayed in Figs. 1-9. The actual state and its fusion estimation are shown in Fig. 1, where the solid curves and dashed curves denote the actual states and the fusion estimations, respectively. The curves of the UB on the FEC for LFs and the fusion filter are plotted in Fig. 2. Then, it can be derived that the ICI fusion filter has better accuracy than any LFs. Meanwhile, the accumulated MSEs for the estimation of the state are shown in Fig. 3, which further tests the performance of the fusion estimation. Based on the changing trends of curves from Fig. 3, it can be seen that the accumulated MSE shows an increasing trend over time, the reasons might depend on many factors, such as measurement noises, delay-dependent nonlinearity, algorithm selection and so on. Because of the statistical characteristic of measurement data, we cannot determine when the accumulated MSE will stop increasing. Furthermore, the behavior of the data will be analyzed to address this issue in future research. Furthermore, it can be easily seen from Fig. 2 and Fig. 3 that UBs locate above their accumulated MSEs. Moreover, Fig. 4 shows that the sensor node is chosen to access the network channel at each moment according to the SCP.

In order to provide the comparison, Fig. 5 shows the traces of the UB of the fusion FEC with the zero-order holder method and zero-input method. It is easy to see that the DFF algorithm with the zero-order holder compensation method has higher estimation precision. In order to show the impact of time-delay d and probability p_i on the performance of the system and evaluate the effectiveness of the proposed method under different scenarios, Fig. 6 shows the traces of the UB of the fusion FEC under different time-delay selections, i.e., $d = 1$, $d = 5$, $d = 7$, and $d = 13$. It can be seen that the trace of the UB increases when the time-delay becomes large. Fig. 7 shows the traces of the UB of the fusion FEC under three probability selections, i.e., $p_1 = 0.1, p_2 = 0.1, p_3 = 0.8$; $p_1 = 0.2, p_2 = 0.2, p_3 = 0.6$; and $p_1 = 0.3, p_2 = 0.3, p_3 = 0.2$. It is easy to see that the probability p_i substantially impacts the overall performance of the proposed method. Meanwhile, it follows from Fig. 3 and Fig. 7 that the higher the probability of the node with the best performance, the better the performance after fusion. However, the performance of the nodes is unknown in practice due to the fact that the SCP is used in network communication to adjust the local node and transmit information in a random way, which may influence the fusion result. As such, the performance of each node can be first evaluated through a small-scale experiment or a simulation by means of the existing data, and then one can establish a feedback loop, where the probability assignments of nodes are updated in terms of the change of the UB with respect to the fusion FEC. Furthermore, for the sake of checking the impact of the fusion rule on the estimation accuracy, Fig. 8 and Fig. 9 depict the traces of the UB on the FEC and accumulated MSEs for DFF algorithm by utilizing ICI fusion rule, CI fusion rule and centralized fusion rule from [15, 34], respectively. In view of the comparison result of simulation, it is clear to see that the estimation accuracy of the provided fusion filter using the ICI fusion rule is better than that using the CI fusion one and lower than centralized fusion one, which further demonstrates the effectiveness of the presented method.

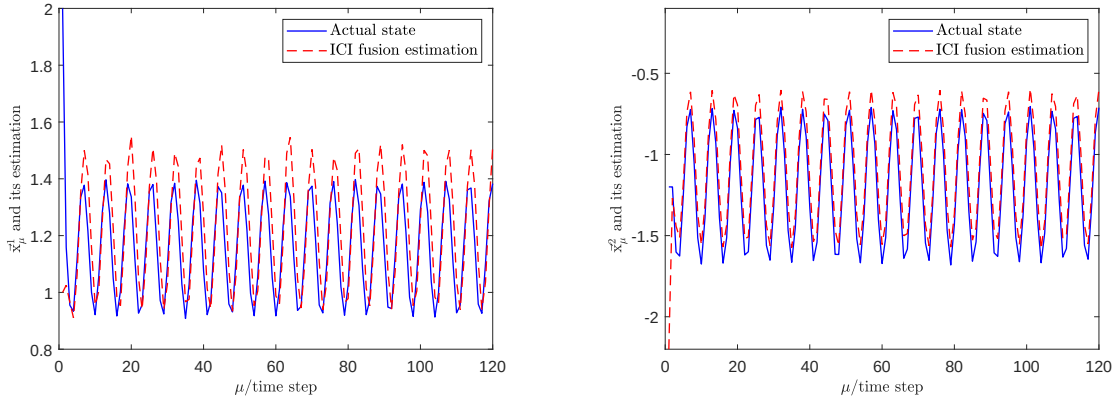

(a) The first component of $\vec{x}_\mu$ (b) The second component of $\vec{x}_\mu$

Figure 1. $\vec{x}_\mu^1$, $\vec{x}_\mu^2$ and their fusion estimations

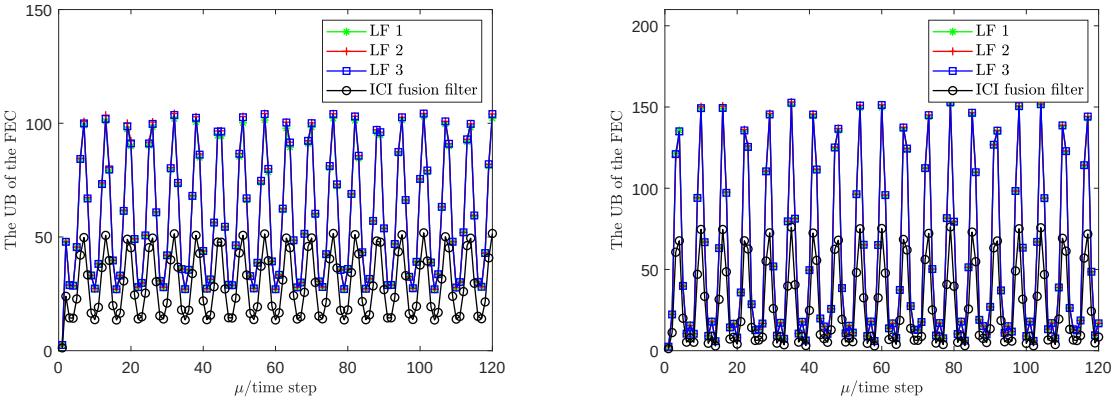

(a) The first component of $\vec{x}_\mu$ (b) The second component of $\vec{x}_\mu$

Figure 2. The UBs of the FEC for the ICI fusion filter and LFs i ($i = 1, 2, 3$)

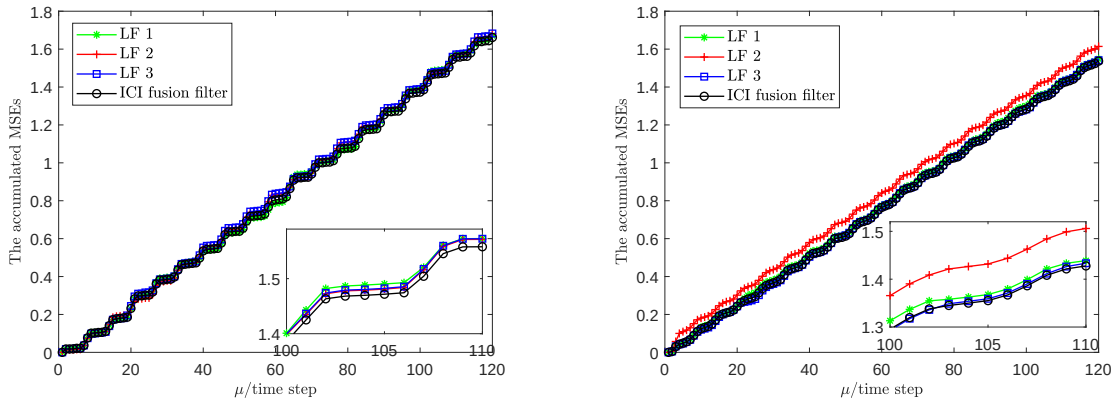

(a) The first component of $\vec{x}_\mu$ (b) The second component of $\vec{x}_\mu$

Figure 3. The accumulated MSEs of the ICI fusion filter and LFs i ($i = 1, 2, 3$)

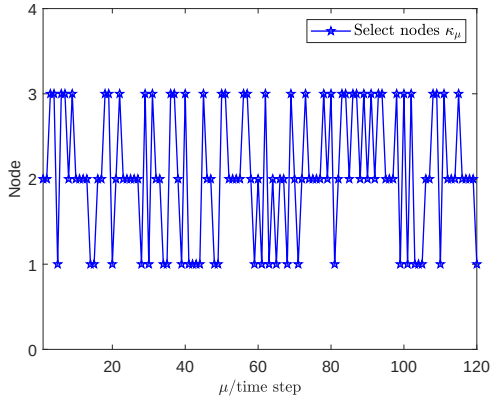

Figure 4. The selection of sensor nodes at each moment

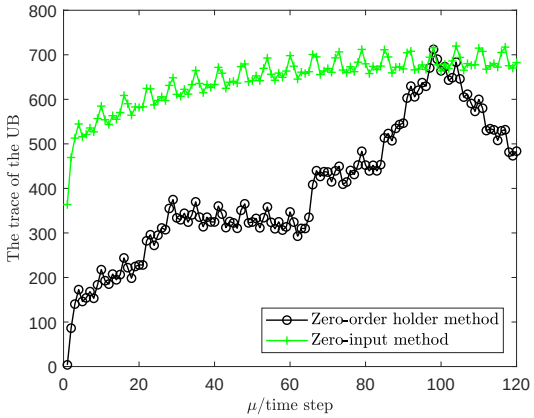

Figure 5. Comparison of the traces of the UB of the fusion FEC under two compensation methods

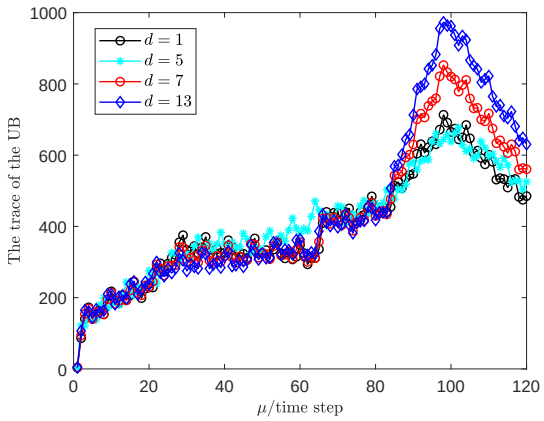

Figure 6. Comparison of the traces of the UB of the fusion FEC under four time-delay selections

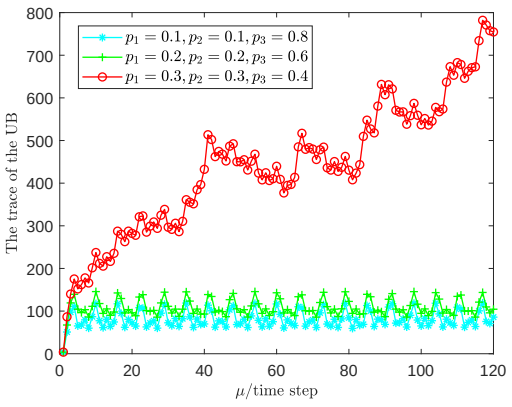

Figure 7. Comparison of the traces of the UB of the fusion FEC under three cases

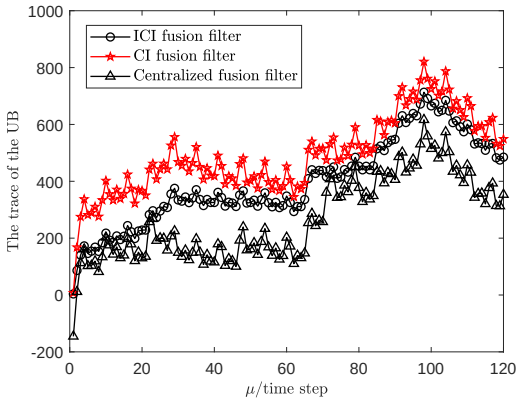

Figure 8. Comparison of the traces of the UB for the DFF algorithm under three fusion filters

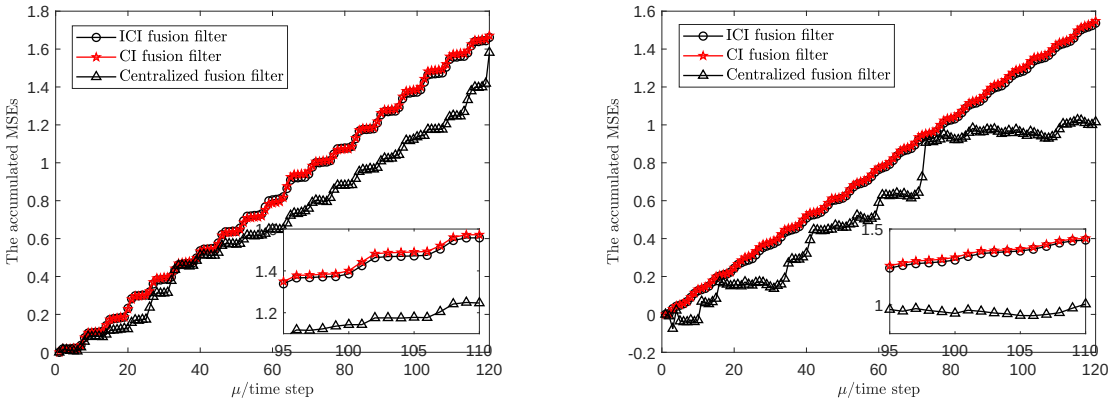

(a) The first component of $\vec{x}_\mu$ (b) The second component of $\vec{x}_\mu$

Figure 9. Comparison of the accumulated MSEs for the DFF algorithm under three fusion filters

5.2. Example 2

Based on the reference [50], we consider the DFF problem for induction machines in this example, and its discretized delayed function $\vec{f}(\vec{\mathrm{x}}_{\mu-1})$ is depicted as

$$\vec{f}(\vec{\mathrm{x}}_{\mu-1}) = \begin{bmatrix} \vec{\mathrm{x}}^1_{\mu-1} + T_k(k_1\vec{\mathrm{x}}^1_{\mu-1} + c_1\vec{\mathrm{x}}^2_{\mu-1} + k_2\vec{\mathrm{x}}^3_{\mu-1} + c_2) \\ \vec{\mathrm{x}}^2_{\mu-1} + T_k(-c_1\vec{\mathrm{x}}^1_{\mu-1} + k_1\vec{\mathrm{x}}^2_{\mu-1} + k_2\vec{\mathrm{x}}^4_{\mu-1}) \\ \vec{\mathrm{x}}^3_{\mu-1} + T_k(k_3\vec{\mathrm{x}}^1_{\mu-1} + k_4\vec{\mathrm{x}}^3_{\mu-1} + (c_1 - \vec{\mathrm{x}}^5_{\mu-1})\vec{\mathrm{x}}^4_{\mu-1}) \\ \vec{\mathrm{x}}^4_{\mu-1} + T_k(k_3\vec{\mathrm{x}}^2_{\mu-1} - (c_1 - \vec{\mathrm{x}}^5_{\mu-1})\vec{\mathrm{x}}^3_{\mu-1} + k_4\vec{\mathrm{x}}^4_{\mu-1}) \\ \vec{\mathrm{x}}^5_{\mu-1} + T_k(k_5(\vec{\mathrm{x}}^1_{\mu-1}\vec{\mathrm{x}}^4_{\mu-1} - \vec{\mathrm{x}}^2_{\mu-1}\vec{\mathrm{x}}^3_{\mu-1})\vec{\mathrm{x}}^2_{\mu-1} + k_6c_3) \end{bmatrix}.$$

Here, $\vec{\mathrm{x}}_\mu = \begin{bmatrix} \vec{\mathrm{x}}^1_\mu & \vec{\mathrm{x}}^2_\mu & \vec{\mathrm{x}}^3_\mu & \vec{\mathrm{x}}^4_\mu & \vec{\mathrm{x}}^5_\mu \end{bmatrix}^T$ is the system state, where $\vec{\mathrm{x}}^1_\mu$, $\vec{\mathrm{x}}^2_\mu$ and $\vec{\mathrm{x}}^3_\mu$, $\vec{\mathrm{x}}^4_\mu$ represent the stator currents and rotor fluxes, respectively. $\vec{\mathrm{x}}^5_\mu$ is the angular velocity. c_1, c_2, c_3 denote the frequency and the amplitude of the stator voltage, and the load torque. The parameters are selected as $k_1 = 0.9814$, $k_2 = 0.0178$, $k_3 = 0.0225$, $k_4 = 0.9766$, $k_5 = -0.0081$, $k_6 = 4,643$, $c_1 = c_2 = 0.1$, and $c_3 = 0$. The other parameters are set as $\vec{A}_\mu = 0$, $\vec{B}_\mu = \begin{bmatrix} 0.01 & 0.02 & 0.01 & 0.091 & 0.05 + 0.01\cos(0.2\mu) \end{bmatrix}^T$, $\vec{C}_{1,\mu} = \begin{bmatrix} 4.448 & 0 & 1 & 0 & 0 \end{bmatrix}$, $\vec{C}_{2,\mu} = \begin{bmatrix} 0 & 4.448 & 0 & 1 & 0 \end{bmatrix}$, $\eta_1 = \eta_2 = \eta_3 = 0.1$, $U_{i,\mu-d} = 0.1I$, $M_{i,\mu-d} = 0.1I$, $\varepsilon_{i,\mu-d} = [1.5\lambda_{\max}(M_{i,\mu-d}\Pi_{i,\mu-d|\mu-d}M^T_{i,\mu-d}) + 1]^{-1}$, and the time-delay is selected as $d = 1$. $\vec{w}_\mu$ and $\vec{v}_{i,\mu}$ $(i = 1, 2)$ are zero-mean noises and their variances are $\vec{Q}_\mu = 1.91$, $R_{1,\mu} = 0.31$ and $R_{2,\mu} = 1.232$, respectively. Besides, let $\Theta_{i,\mu} = \mathrm{diag}\left\{\theta^{(1)}_{i,\mu}\right\}$ $(i = 1, 2)$, where the probability mass function for $\theta^{(1)}_{i,\mu}$ satisfies

$$\mathrm{Prob}\{\theta^{(1)}_{i,\mu} = s\} = \begin{cases} 0.2, & s = 0, \\ 0.4, & s = 0.4, \\ 0.4, & s = 1, \end{cases}$$

so their expectations and variances are easily derived as $\bar{\theta}^{(1)}_{i,\mu} = 0.56$ and $\rho^{(1)}_{i,\mu} = 0.1504$, respectively. The initial values are set as $\bar{\vec{\mathrm{x}}}_{-1} = \bar{\vec{\mathrm{x}}}_0 = \begin{bmatrix} 0.01 & 0.02 & 0.01 & -0.01 & 0.01 \end{bmatrix}^T$, $\hat{\mathrm{x}}_{i,-1|-1} = \hat{\mathrm{x}}_{i,0|0} = \begin{bmatrix} \bar{\vec{\mathrm{x}}}^T_0 & 0^T \end{bmatrix}^T$, $\vec{P}_{-1|-1} = \vec{P}_{0|0} = 1.2I$, $\Pi_{i,-1|-1} = \Pi_{i,0|0} = 1.2I$. Next, for SCP, the probabilities of each sensor to be selected are given as $\mathrm{Prob}\left\{\kappa_\mu = 1\right\} = 0.3$ and $\mathrm{Prob}\left\{\kappa_\mu = 2\right\} = 0.7$. Based on the above parameters, Fig. 10 plots the accumulated MSEs for LFs and fusion filter. It can be seen that the accumulated MSE of the fusion filter is better than that the LFs. Fig. 11 shows the logarithm of trace of UBs of the FEC for ICI fusion filter and LFs. From Fig. 11, it is clear that the estimation accuracy of the ICI fusion filter is superior to that of the LFs. The simulation results further check the feasibility of the presented DFF method.

Remark 7 *In view of the theoretical analysis of the Theorem 3 and two examples, the detailed theoretical investigations including rigorous derivations and mathematical proof have been given to evaluate the conservativeness of the UB. Specifically, depending on the certain assumption condition, the uniform boundedness with respect to the UB has been ensured via providing a sufficient condition, which presents an effective approach to determine the tightness of the UB. In addition, in order to show the performance of the proposed approach, the numerical and practical simulations have been provided. From these simulation results, we can see that the conservativeness of the UB on fusion accuracy is influenced by time-delay d, probability p_i, fusion rules and so on. In addition, it can be seen from above simulation results that the initial value of the accumulated MSE is set zero based on the initial conditions selection of the system state in order to simplify the initialization process and more clearly demonstrate the performance of the developed algorithm. Meanwhile, due to the accumulated MSE being a cumulative summing approach, the divergence of the accumulated MSE appears in simulation results over time, which can be attributed to various factors, including the nonlinear characteristics of the model, system noises, SCP and so on. As such, a more robust fusion estimation strategy needs to be further developed to address these issues in the future.*

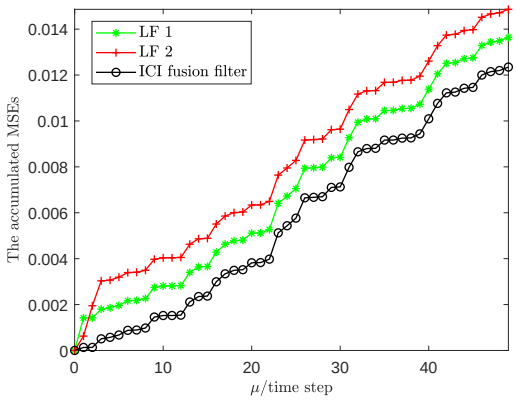

(a) The first component of $\vec{x}_\mu$

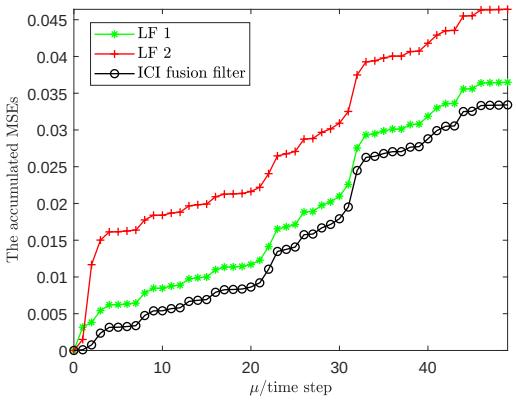

(b) The second component of $\vec{x}_\mu$

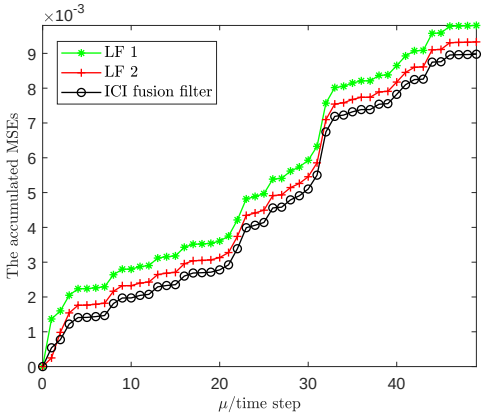

(c) The third component of $\vec{x}_\mu$

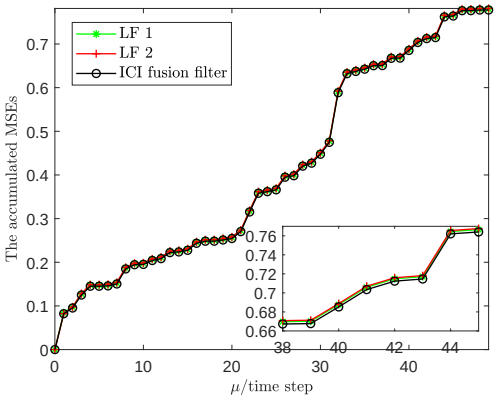

(d) The fourth component of $\vec{x}_\mu$

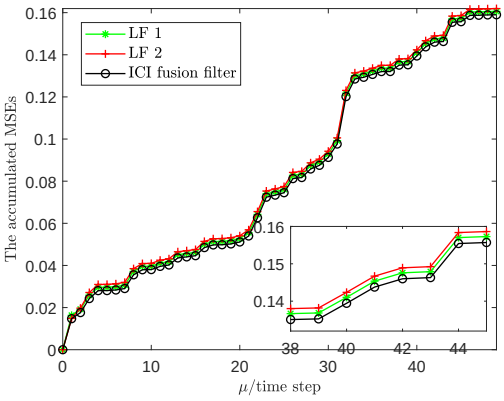

(e) The fifth component of $\vec{x}_\mu$

Figure 10. Comparison of the accumulated MSEs of the ICI fusion filter and LFs

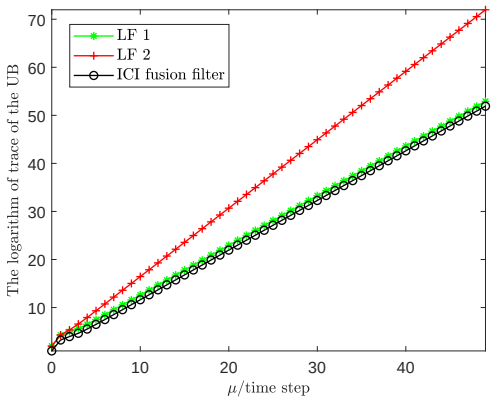

Figure 11. Comparison of the logarithm of trace of UBs of the FEC on the ICI fusion filter and LFs

6. Conclusions

In this paper, we have discussed the DFF problem for a class of nonlinear delayed MSNSs in the presence of MFMs and SCP. For each sensor node, a diagonal matrix with independent stochastic elements has been utilized to depict the phenomenon of MFMs, and SCP has been employed to save network resources and reduce network congestion. By means of the stochastic analysis technique as well as the induction approach, a local UB on the FEC have been deduced, and then the LF gain has been calculated to ensure the minimized UB. In addition, a sufficient condition has been presented to guarantee the boundedness of the local UB regarding the FEC. Finally, a simulation example has been used to illustrate that the feasibility of the proposed DFF scheme has been verified. Furthermore, when the sensing abilities and channel load of sensors are different, it may result in uneven data collection and then affect the whole performance. Hence, the further extension of DFF method by considering the sensing abilities and channel load of sensors remains an interesting research topic in the future.

Acknowledgments

This work was supported in part by the National Natural Science Foundation of China under Grants 12171124, the Natural Science Foundation of Heilongjiang Province of China under Grant ZD2022F003, the National High-end Foreign Experts Recruitment Plan of China under Grant G2023012004L, the MCIN/AEI/ 10.13039/501100011033 and "ERDF A way of making Europe" under Grant PID2021-124486NB-I00, and the Alexander von Humboldt Foundation of Germany.

References

[1] Y. Qiu, H. Zhang, and K. Long, Computation offloading and wireless resource management for healthcare monitoring in fog-computing based internet of medical things, *IEEE Internet of Things Journal*, vol. 8, no. 21, pp. 15875–15883, 2021.

[2] M. Sadeghi, F. Behnia, and R. Amiri, Optimal geometry analysis for TDOA–based localization under communication constraints, *IEEE Transactions on Aerospace and Electronic Systems*, vol. 57, no. 5, pp. 3096–3106, 2021.

[3] Y. Yuan, X. Liu, W. Li, W. Yi, and W. Choi, Decentralized resource allocation for multi-radar systems based on quality of service framework, *IEEE Transactions on Signal Processing*, vol. 72, pp. 1189–1204, 2024.

[4] Y. Yuan, W. Yi, W. Choi, and L. Kong, Dynamic quantizer design for target tracking for wireless sensor network with imperfect channels, *IEEE Transactions on Wireless Communications*, vol. 22, no. 3, pp. 1695–1711, 2023.

[5] F. Qu, X. Zhao, X. Wang, and E. Tian, Probabilistic-constrained distributed fusion filtering for a class of time-varying systems over sensor networks: A torus-event-triggering mechanism, *International Journal of Systems Science*, vol. 53, no. 6, pp. 1288–1297, 2022.

[6] J. R. Cano, J. Luengo, and S. García, Label noise filtering techniques to improve monotonic classification, *Neurocomputing*, vol. 353, pp. 83-95, 2019.

[7] M. Gonz¢lez, G. González-Almagro, I. Triguero, J. R. Cano, and S. García, Decomposition-fusion for label distribution learning, *Information Fusion*, vol. 66, pp. 64–75, 2021.

[8] R. Caballero-Águila, A. Hermoso-Carazo, and J. Linares-Pérez, Networked distributed fusion estimation under uncertain outputs with random transmission delays, packet losses and multi-packet processing, *Signal Processing*, vol. 156, pp. 71–83, 2019.
[9] R. Caballero-Águila and J. Linares-Pérez, Distributed fusion filtering for uncertain systems with coupled noises, random delays and packet loss prediction compensation, *International Journal of Systems Science*, vol. 54, no. 2, pp. 371–390, 2023.
[10] S. Sun, Distributed optimal linear fusion estimators, *Information Fusion*, vol. 63, pp. 56–73, 2020.
[11] H. Jin and S. Sun, Distributed filtering for multi-sensor systems with missing data, *Information Fusion*, vol. 86–87, pp. 116–135, 2022.
[12] J. Ma and S. Sun, Globally optimal distributed and sequential state fusion filters for multi-sensor systems with correlated noises, *Information Fusion*, vol. 99, Article number: 101885, 2023.
[13] H. Lin and S. Sun, Globally optimal sequential and distributed fusion state estimation for multi-sensor systems with cross-correlated noises, *Automatica*, vol. 101, pp. 128–137, 2019.
[14] B. Noack, J. Sijs, M. Reinhardt, and U. D. Hanebeck, Decentralized data fusion with inverse covariance intersection, *Automatica*, vol. 79, pp. 35–41, 2017.
[15] D. Yu, Y. Xia, L. Li, Z. Xing, and C. Zhu, Distributed covariance intersection fusion estimation with delayed measurements and unknown inputs, *IEEE Transactions on Systems, Man, and Cybernetics: Systems*, vol. 51, no. 8, pp. 5165–5173, 2021.
[16] W. Lin, Y. He, C. Zhang, and M. Wu, Stochastic finite-time H_∞ state estimation for discrete-time semi-Markovian jump neural networks with time-varying delays, *IEEE Transactions on Neural Networks and Learning Systems*, vol. 31, no. 12, pp. 5456–5467, 2020.
[17] É. Gyurkovics and T. Takács, Multiple integral inequalities and stability analysis of time delay systems, *Systems and Control Letters*, vol. 96, pp. 72–80, 2016.
[18] H. Jin and S. Sun, Distributed filtering for sensor networks with fading measurements and compensations for transmission delays and losses, *Signal Processing*, vol. 190, Article number: 108306, 2022.
[19] C. Ran and Z. Deng, Robust fusion Kalman estimators for networked mixed uncertain systems with random one-step measurement delays, missing measurements, multiplicative noises and uncertain noise variances, *Information Sciences*, vol. 534, pp. 27–52, 2020.
[20] S. Li, Y. Chen, and J. Zhan, Event-triggered consensus control and fault estimation for time-delayed multi-agent systems with Markov switching topologies, *Neurocomputing*, vol. 460, pp. 292–308, 2021.
[21] F. Han, D. Ding, F. Yang, and W. Gao, Distributed resilient estimation over sensor networks for nonlinear time-delayed systems with stochastic perturbations, *International Journal of Robust and Nonlinear Control*, vol. 30, no. 3, pp. 843–863, 2020.
[22] L. Ma, Z. Wang, Y. Liu, and F. E. Alsaadi, Distributed filtering for nonlinear time-delay systems over sensor networks subject to multiplicative link noises and switching topology, *International Journal of Robust and Nonlinear Control*, vol. 29, no. 10, pp. 2941–2959, 2019.
[23] L. Liu, L. Ma, J. Guo, J. Zhang, and Y. Bo, Distributed set-membership filtering for time-varying systems: A coding-decoding-based approach, *Automatica*, 2021, vol. 129, article no. 109684, DOI:10.1016/j.automatica.2021.109684.
[24] S. Sun, H. Lin, J. Ma, and X. Li, Multi-sensor distributed fusion estimation with applications in networked systems: A review paper, *Information Fusion*, vol. 38, pp. 122–134, 2017.
[25] W. L. De Koning, Optimal estimation of linear discrete-time systems with stochastic parameters, *Automatica*, vol. 20, no. 1, pp. 113–115, 1984.
[26] X.-M. Zhang, Q.-L. Han, and X. Ge, A novel approach to H_∞ performance analysis of discrete-time networked systems subject to network-induced delays and malicious packet dropouts, *Automatica*, vol. 136, Article number: 110010, 2022.
[27] J. Hu, L. Zuo, V. K. Pramod, and Y. Gao, Resource allocation for distributed multi-target tracking in radar networks with missing data, *IEEE Transactions on Signal Processing*, vol. 72, pp. 718–734, 2024.
[28] Y. Shen and S. Sun, Distributed recursive filtering for multi-rate uniform sampling systems with packet losses in sensor networks, *International Journal of Systems Science*, vol. 54, no. 8, pp. 1729–1745, 2023.
[29] D. Ding, Q.-L. Han, X. Ge, and J. Wang, Secure state estimation and control of cyber-physical systems: A survey, *IEEE Transactions on Systems, Man, and Cybernetics: Systems*, vol. 51, no. 1, pp. 176–190, 2021.
[30] H. Yuan and Y. Xia, Secure filtering for stochastic non-linear systems under multiple missing measurements and deception attacks, *IET Control Theory and Applications*, vol. 12, no. 4, pp. 515–523, 2018.
[31] J. Hu, Z. Hu, R. Caballero-Águila, C. Chen, S, Fan, and X. Yi , Distributed resilient fusion filtering for nonlinear systems with multiple missing measurements via dynamic event-triggered mechanism, *Information Sciences*, vol. 637, Article number: 118950, 2023.
[32] S. Sun, T. Tian, and H. Lin, State estimators for systems with random parameter matrices, stochastic nonlinearities, fading measurements and correlated noises, *Information Sciences*, vol. 397, pp. 118–136, 2017.
[33] J. Hu, Z. Wang, and H. Gao, Recursive filtering with random parameter matrices, multiple fading measurements and correlated noises, *Automatica*, vol. 49, no. 11, pp. 3440–3448, 2013.
[34] H. Lin and S. Sun, Optimal sequential fusion estimation with stochastic parameter perturbations, fading measurements, and correlated noises, *IEEE Transactions on Signal Processing*, vol. 66, no. 13, pp. 3571–3593, 2018.
[35] H. Lin and S. Sun, Estimation for networked random sampling systems with packet losses, *IEEE Transactions on Systems Man Cybernetics: Systems*, vol. 51, no. 9, pp. 5511–5521, 2021.
[36] R. Sakthivel, O.-M. Kwon, M. J. Park, R. Sakthivel, Event-triggered finite-time dissipative filtering for interval Type-2 fuzzy complex dynamical networks with cyber attacks, *IEEE Transactions on Systems Man Cybernetics-Systems*, vol. 53, no. 5, pp. 3042–3053, 2023.
[37] Y. Shen, Z. Wang, B. Shen, and H. Dong, Outlier-resistant recursive filtering for multisensor multirate networked systems under weighted try-once-discard protocol, *IEEE Transactions on Cybernetics*, vol. 51, no. 10, pp. 4897–4908, 2021.
[38] Y. Ju, D. Ding, X. He, Q.-L. Han, and G. Wei, Consensus control of multi-agent systems using fault-estimation-in-the-loop: dynamic event-triggered case, *IEEE/CAA Journal of Automatica Sinica*, vol. 9, no. 8, pp. 1440–1451, 2022.
[39] L. Orihuela, F. Gómez-Estern, and F. Rodríguez Rubio, Scheduled communication in sensor networks, *IEEE Transactions on Control Systems Technology*, vol. 22, no. 2, pp. 801–808, 2013.
[40] H. Tan, B. Shen, Q. Li, and H. Liu, Recursive filtering for stochastic systems with filter-and-forward successive relays, *IEEE/CAA Journal of Automatica Sinica*, vol. 11, no. 5, pp. 1202–1212, 2024.
[41] H. Liu, Z. Wang, W. Fei, J. Li, and F. E. Alsaadi, On finite-horizon H_∞ state estimation for discrete-time delayed memristive neural networks

under stochastic communication protocol, *Information Sciences*, vol. 555, pp. 280–292, 2021.
[42] Y. Luo, Z. Wang, Y. Chen, and X. Yi, H_∞ state estimation for coupled stochastic complex networks with periodical communication protocol and intermittent nonlinearity switching, *IEEE Transactions on Network Science and Engineering*, vol. 8, no. 2, pp. 1414–1425, 2021.
[43] X. Wan, Z. Wang, Q.-L. Han, and M. Wu, A recursive approach to quantized H_∞ state estimation for genetic regulatory networks under stochastic communication protocols, *IEEE Transactions on Neural Networks and Learning Systems*, vol. 30, no. 9, pp. 2840–2852, 2019.
[44] H. Zhou and S. Sun, Distributed filtering for multi-sensor networked systems with stochastic communication protocol and correlated noises, *Information Fusion*, vol. 104, Article number: 102121, 2024.
[45] H. Geng, Z. Wang, J. Hu, H. Dong, and Y. Cheng, Distributed recursive filtering over sensor networks under random access protocol: When state saturation meets censored measurement, *IEEE Transactions on Cybernetics*, vol. 53, no. 12, pp. 7760–7772, 2023.
[46] L. Zou, Z. Wang, Q.-L. Han, and D. Zhou, Moving horizon estimation of networked nonlinear systems with random access protocol, *IEEE Transactions on Systems, Man, and Cybernetics: Systems*, vol. 51, no. 5, pp. 2937–2948, 2021.
[47] L. Zou, Z. Wang, Q.-L. Han, and D. Zhou, Recursive filtering for time-varying systems with random access protocol, *IEEE Transactions on Automatic Control*, vol. 64, no. 2, pp. 720–727, 2018.
[48] R. A. Horn and C. R. Johnson, Topic in matrix analysis, New York: Cambridge University Press, 1991.
[49] Y. Wang, L. Xie, and C. E. de Souza, Robust control of a class of uncertain nonlinear systems, *Systems and Control Letters*, vol. 19, no. 2, pp. 139–149, 1992.
[50] S. Liu, Z. Wang, J. Hu, and G. Wei, Protocol-based extended Kalman filtering with quantization effects: The Round-Robin case, *International Journal of Robust and Nonlinear Control*, vol. 30, no. 18, pp. 7927–7946, 2020.